Received: 15 February 2021 | Revised: 28 July 2021 | Accepted: 30 July 2021

DOI: 10.1002/nme.6801

RESEARCH ARTICLE

WILEY

A nonsmooth generalized-alpha method for mechanical systems with frictional contact

Giuseppe Capobianco | **Jonas Harsch** | **Simon R. Eugster** | **Remco I. Leine**

Institute for Nonlinear Mechanics, University of Stuttgart, Stuttgart, Germany

Correspondence
Giuseppe Capobianco, Institute for Nonlinear Mechanics, University of Stuttgart, Pfaffenwaldring 9, 70569 Stuttgart, Germany.
Email: capobianco@inm.uni-stuttgart.de

Abstract

In this article, the existing nonsmooth generalized-α method for the simulation of mechanical systems with frictionless contacts, modeled as unilateral constraints, is extended to systems with frictional contacts. On that account, we complement the unilateral constraints with set-valued Coulomb-type friction laws. Moreover, we devise a set of benchmark systems, which can be used to validate numerical schemes for mechanical systems with frictional contacts. Finally, this set of benchmarks is used to numerically assert the properties striven for during the derivation of the presented scheme. Specifically, we show that the presented scheme can reproduce the dynamics of the frictional contact adequately and no numerical penetration of the contacting bodies arises—a big issue for most popular time-stepping schemes such as the one of Moreau. Moreover, we demonstrate that the presented scheme performs well for multibody systems containing flexible parts and that it allows general parametrizations such as the use of unit quaternions for the rotation of rigid bodies.

KEYWORDS

Coulomb friction, flexible multibody system, nonsmooth contact dynamics, time-stepping scheme, unilateral constraint

1 | INTRODUCTION

In this article, we derive a nonsmooth generalized-α method for the simulation of mechanical systems with *frictional* contact. Moreover, we introduce a set of benchmark systems to validate the presented scheme.

In many engineering applications, systems are modeled through rigid and flexible bodies, which are interconnected by joints and can come into contact with each other or their surroundings. Prominent examples are automotive and robotic systems. The dynamics of mechanical systems with frictional contact can be described within the theory of nonsmooth mechanics,[1,2] where the velocities of the system are allowed to jump. This is particularly important for the description of contact between rigid bodies, where at the time instant when the contacting bodies touch, an impact might occur, which due to rigidity instantaneously changes the velocity of the body.

For the simulation of nonsmooth mechanical systems, two approaches can be distinguished, the event-driven and the event-capturing schemes. The event-driven schemes use standard ordinary differential equations (ODE) solvers, or differential algebraic equations (DAE) solvers, to compute the impact-free motion. Every time an impact event

is detected, the algebraic impact equations are solved to find the postimpact velocities, which are then used to continue the integration with the ODE solver. The main strength of event-driven integration is that ODE solvers with high-order accuracy can be used. However, since every impact is resolved, these schemes are not suitable to find motions with accumulation points, that is, motions with an infinite number of impacts occurring in a finite interval of time.

In contrast to event-driven schemes, the event-capturing schemes, also called time-stepping schemes, can overcome accumulation points, because they smear the effects of impacts over a time step. However, the most widespread schemes, such as Moreau's time-stepping scheme[1] and variants thereof, are of first-order accuracy, show a high level of numerical dissipation and allow penetration of the contacting bodies. These properties are problematic, especially for the simulation of mechanical systems containing elastic parts. Several publications present improved event-capturing schemes by addressing at least one of these drawbacks. In References 3,4, integrators similar to Moreau's time-stepping scheme with improved long-term energy behavior have been derived. To arrive at event-capturing schemes with higher accuracy order for the impact-free motion, Reference 5 combines high-order Runge–Kutta methods with Moreau's time-stepping scheme, Reference 6 relies on extrapolation methods, and Reference 7 uses a discontinuous Galerkin method to discretize the dynamics of the mechanical system. The constraint drift, which is also responsible for contact penetration, is generally solved by a stabilization in the sense of Gear–Gupta–Leimkuhler (GGL)[8] and/or a projection approach, see, for example, References 9,10.

In References 11-14, the nonsmooth generalized-α methods were introduced, which alleviate many of the problems of the Moreau-type time-stepping schemes. In particular, the generalized-α schemes are second-order accurate for the impact-free motion, use the GGL stabilization to avoid penetration of the contacting bodies and it is known from structural mechanics applications, see References 15-17, that generalized-α schemes perform well for flexible multibody systems. However, the nonsmooth generalized-α methods of References 11-14 are only applicable to multibody systems with frictionless contacts, that is, unilateral constraints without Coulomb friction. Furthermore, these nonsmooth generalized-α methods are restricted to mechanical systems for which the velocity of the system corresponds to the time derivative of the position coordinates. In References 18,19, the schemes of References 11-14 have been extended to cope with systems with frictional contact and a more general kinematic equation. In Reference 18, the augmented Lagrangian approach together with discrete set-valued Coulomb friction laws on position and velocity level have been used to arrive at a nonsmooth generalized-α scheme, which can describe systems with frictional contact. The scheme of Reference 18 has been extended in Reference 19 to allow for different rotation parametrizations for rigid bodies. This represents a particular case of a general kinematic equation since the angular velocity is not the time derivative of the rotation matrix describing the orientation of a rigid body. The nonsmooth generalized-α methods of References 11-14,18,19 are derived from a splitting strategy, where the motion is artificially split into a nonsmooth and a smooth part. Furthermore, the contact laws describing the impenetrability of the contacting bodies (Signorini condition) as well as the impact between these bodies (Newton's impact law) are introduced either as inequality complementarity conditions or equivalently as normal cone inclusions. The discrete counterparts of the contact laws are given as an active set formulation, that is, depending on the state of the system, conditions are established that decide which set of nonlinear equations describes the contact. This set of nonlinear equations is finally solved by a semismooth Newton method in every time step.

In nonsmooth mechanics, the set-valued Coulomb friction law is naturally stated as a force law on velocity level. Since in the case of sticking this friction law acts like a bilateral constraint, it can be brought to acceleration level through differentiation. Similar to References 18,19, it is the aim of this article to extend the nonsmooth generalized-α schemes[11-14] to account for friction as well as a general kinematic equation. However, the explained link between the friction law on velocity and acceleration level will be exploited instead of formulating the discrete friction laws on position and velocity level as done in References 18,19.

We use the same generalized-α time discretization for the dynamics of the mechanical system as the schemes of References 11-14, but include the general kinematic equation. In doing so, the presented scheme shares the beneficial properties of the existing generalized-α schemes, such as the second-order accuracy and the absence of numerical contact penetration. To account for friction, we invoke set-valued Coulomb-type friction laws introduced as normal cone inclusions. We exploit the fact that also the Signorini condition and Newton's impact law can be formulated as normal cone inclusions, such that the contact laws are given as a set of normal cone inclusions. We directly discretize these contact laws to arrive at their discrete counterparts, which are again a set of normal cone inclusions. This opens the possibility to numerically solve the time step using any strategy suitable for the solution of normal cone inclusion problems, see, for example, Reference 20. We present two such strategies, which both rely on a reformulation of the normal cone

inclusion invoking the proximal point function to arrive at implicit nonlinear equations. For the first strategy, the proximal point function is used to achieve an active set formulation of the contact laws, which are then solved by a semismooth Newton method. The second strategy solves the nonlinear equations including the proximal point functions with fixed point iterations. Finally, we introduce a set of benchmark systems, which can be used to validate numerical schemes for mechanical systems with frictional contacts. Therefore, we devise the systems in such a way, that each benchmark can be used to test the performance of the scheme with respect to a specific feature. These are overcoming accumulation points, slip-stick transitions, handling the presence of linearly dependent force directions, contact penetration, the Painlevé paradox, the suitability of the scheme for the simulation of flexible multibody systems, combined spatial friction laws and general kinematic equations. We use these benchmark systems, to validate the performance of the presented scheme.

The mathematical concepts used for the discretization of the contact laws as well as their numerical treatment is presented in Section 2. In Section 3, the equations of motion of a mechanical system subjected to ideal bilateral constraints as well as frictional contacts are established. To avoid that the resulting generalized-α scheme exhibits numerical constraint drift, and hence penetration of the contacting bodies, a constraint stabilization in the sense of Gear–Gupta–Leimkuhler is introduced in Section 4. Subsequently, the generalized-α discretization of the dynamics is presented in Section 5, the contact laws in normal direction of the contacting surfaces of the bodies are discretized in Section 6 and the discretization of the friction laws is conducted in Section 7. The extension to general relations between velocities and position is discussed in Section 8. The reformulation of the discrete contact laws as nonlinear equations and how these are solved with a semismooth Newton method or fixed point iterations is shown in Section 9. Finally, a set of mechanical benchmark systems is used to validate the derived nonsmooth generalized-α scheme in Section 10.

2 | MATHEMATICAL PRELIMINARIES

2.1 | Convex sets and cones

A set $C \subseteq \mathbb{R}^n$ is convex if and only if $\alpha\ \mathbf{a} + (1-\alpha)\mathbf{b} \in C$ for all $\mathbf{a}, \mathbf{b} \in C$ and for all $\alpha \in [0,1]$. For $\lambda \in \mathbb{R}$, we introduce the scalar multiple of a set $C \subseteq \mathbb{R}^n$ as $\lambda C = \{\lambda \mathbf{x}\ |\mathbf{x} \in C\}$. If C is convex then it holds that

$$\mathbf{x}_1 \in \alpha_1 C, \quad \mathbf{x}_2 \in \alpha_2 C \quad \Rightarrow \quad \mathbf{x}_1 + \mathbf{x}_2 \in (\alpha_1 + \alpha_2) C \tag{1}$$

for $\alpha_1, \alpha_2 \geq 0$. More generally, it holds for a closed convex set C that

$$\mathbf{x}_i \in \alpha_i\ C, \quad i = 1, 2, 3, \ldots \quad \Rightarrow \quad \sum_i \mathbf{x}_i \in \left(\sum_i \alpha_i \right) C, \tag{2}$$

where $\alpha_i \geq 0$.

Let $K \subseteq \mathbb{R}^n$ be a cone, that is, the set K fulfills the cone property

$$\mathbf{a} \in K \quad \Rightarrow \quad \alpha\ \mathbf{a} \in K \quad \forall \alpha > 0. \tag{3}$$

For a closed cone K it holds that when $\mathbf{a} \in K$ also $\alpha\ \mathbf{a} \in K$ for all $\alpha \geq 0$. Moreover, if K is a closed convex cone, then it holds that

$$\mathbf{a}_i \in K, \quad i = 1, 2, 3, \ldots \quad \Rightarrow \quad \sum_i \mathbf{a}_i \in K, \tag{4}$$

and, likewise,

$$\mathbf{a}(t) \in K \quad \forall t \in I \quad \Rightarrow \quad \int_I \mathbf{a}(t)\ \mathrm{d}t \in K, \tag{5}$$

where $I \subseteq \mathbb{R}$ and the Lebesgue measure $\mathrm{d}t$ may be generalized to any positive measure.

2.2 | Properties of normal cones

Let $C \subseteq \mathbb{R}^n$ be a closed convex nonempty set. The normal cone of C at $\mathbf{x} \in C$ is defined as

$$\mathcal{N}_C(\mathbf{x}) = \{\mathbf{y} \in C \mid \mathbf{y}^{\mathrm{T}}(\mathbf{x}^* - \mathbf{x}) \leq 0, \forall \mathbf{x}^* \in C\}, \tag{6}$$

whereas $\mathcal{N}_C(\mathbf{x})$ is empty if $\mathbf{x} \notin C$. One can show that the normal cone $\mathcal{N}_C(\mathbf{x})$ is a closed convex cone, see Reference 21. It can easily be verified, that $\mathcal{N}_C(\mathbf{x}) = \{0\}$ if $\mathbf{x}$ is an interior point of the set C. Indeed, for an interior point $\mathbf{x}$ there exists a ball around $\mathbf{x}$ contained in C. This allows to choose $\mathbf{x}^*$ from this ball such that any direction $\mathbf{x}^* - \mathbf{x}$ can be produced in (6), which leaves only $\mathbf{y} = 0$ to fulfill the inequality.

The normal cone has a number of less known scaling properties needed in this article. These may conveniently be proved using topics from convex analysis such as the subdifferential and the support function. However, here we will try to introduce as little machinery as possible and derive these properties by using only the definition (6).

Proposition 1. *Let $\alpha > 0$ and C be a closed convex nonempty set. It then holds that*

$$\mathbf{y} \in \mathcal{N}_{\alpha C}(\mathbf{x}) \quad \Leftrightarrow \quad \mathbf{y} \in \mathcal{N}_C\left(\frac{1}{\alpha}\mathbf{x}\right). \tag{7}$$

Proof. Consider $\mathbf{x} \in \alpha C$. The definition (6) applied on the inclusion $\mathbf{y} \in \mathcal{N}_{\alpha C}(\mathbf{x})$ implies that $\mathbf{y}^{\mathrm{T}}(\mathbf{x}^* - \mathbf{x}) \leq 0, \forall \mathbf{x}^* \in \alpha C$. We divide by $\alpha > 0$ giving

$$\mathbf{y}^{\mathrm{T}}\left(\frac{1}{\alpha}\mathbf{x}^* - \frac{1}{\alpha}\mathbf{x}\right) \leq 0 \quad \forall \frac{1}{\alpha}\mathbf{x}^* \in C \quad \Leftrightarrow \quad \mathbf{y} \in \mathcal{N}_C\left(\frac{1}{\alpha}\mathbf{x}\right). \tag{8}$$

Furthermore, $\mathbf{x} \notin \alpha C$ implies $\mathcal{N}_{\alpha C}(\mathbf{x}) = \emptyset$, which in turn yields $\mathcal{N}_C\left(\frac{1}{\alpha}\mathbf{x}\right) = \emptyset$. The other direction of the implication follows by taking the reciprocal value of α. ∎

Proposition 2. *Let C be a closed convex nonempty set and $C(\alpha) = \alpha C$ for all $\alpha \geq 0$. If*

$$\mathbf{y} \in \mathcal{N}_{C(\alpha_i)}(\mathbf{x}_i), \quad i = 1, 2, 3 \ \ldots\ , \tag{9}$$

where $\alpha_i \geq 0$, then it holds that

$$\mathbf{y} \in \mathcal{N}_{C\left(\sum_i \alpha_i\right)}\left(\sum_i \mathbf{x}_i\right). \tag{10}$$

Proof. Retaining the case $\alpha_i = 0$ for the end of the proof, we first consider $\alpha_i > 0$ for all i. By using Proposition 1 together with the homogeneity $C(\alpha) = \alpha C(1) = \alpha C$ we infer from $\mathbf{y} \in \mathcal{N}_{C(\alpha_i)}(\mathbf{x}_i)$, that

$$\mathbf{y} \in \mathcal{N}_C\left(\frac{1}{\alpha_i}\mathbf{x}_i\right), \quad i = 1, 2, 3 \ \ldots\ . \tag{11}$$

Without loss of generality, consider $i = 1, 2$ and use the definition (6) for either, that is,

$$\mathbf{y}^{\mathrm{T}}\left(\frac{1}{\alpha_1}\mathbf{x}_1^* - \frac{1}{\alpha_1}\mathbf{x}_1\right) \leq 0 \quad \forall \frac{1}{\alpha_1}\mathbf{x}_1^* \in C \tag{12}$$

$$\mathbf{y}^{\mathrm{T}}\left(\frac{1}{\alpha_2}\mathbf{x}_2^* - \frac{1}{\alpha_2}\mathbf{x}_2\right) \leq 0 \quad \forall \frac{1}{\alpha_2}\mathbf{x}_2^* \in C. \tag{13}$$

We now sum the inequalities, but multiply by α_1 and α_2 respectively to arrive at

$$\mathbf{y}^{\mathrm{T}}(\mathbf{x}_1^* + \mathbf{x}_2^* - \mathbf{x}_1 - \mathbf{x}_2) \leq 0 \quad \forall \mathbf{x}^* = \mathbf{x}_1^* + \mathbf{x}_2^* \in (\alpha_1 + \alpha_2)C, \tag{14}$$

where we used property (1) of a convex set C. Repeated summation gives

$$\mathbf{y}^{\mathrm{T}}\left(\sum_i \mathbf{x}_i^* - \sum_i \mathbf{x}_i\right) \leq 0 \quad \forall \mathbf{x}^* = \sum_i \mathbf{x}_i^* \in \left(\sum_i \alpha_i\right) C = C\left(\sum_i \alpha_i\right), \tag{15}$$

which is equivalent to

$$\mathbf{y} \in \mathcal{N}_{C\left(\sum_i \alpha_i\right)} \left(\sum_i \mathbf{x}_i \right). \tag{16}$$

If $\alpha_i = 0$ for some i, then it holds that $C(\alpha_i) = C(0) = \{0\}$ and $\mathbf{x}_i = 0$, whereas $\mathcal{N}_{\{0\}}(0) = \mathbb{R}^n$. One easily verifies that the proposition still holds. ∎

Proposition 2 may also be written in integral form as

$$\mathbf{y} \in \mathcal{N}_{C(\alpha(t))}(\mathbf{x}(t)) \quad \forall t \in I \subseteq \mathbb{R} \quad \Rightarrow \quad \mathbf{y} \in \mathcal{N}_{C\left(\int_I \alpha(t)\mathrm{d}t\right)} \left(\int_I \mathbf{x}(t)\, \mathrm{d}t \right), \tag{17}$$

where $\alpha(t) \geq 0$ and where $\mathbf{y}$ is a fixed value, that is, does not depend on t.

2.3 | Reformulations and numerical solution of normal cone inclusion problems

The generalized-α discretization of the dynamics of mechanical systems with frictional contacts results in a normal cone inclusion problem, that is, a set of nonlinear equations and normal cone inclusions, describing a time step of the scheme. Hence, finding a numerical solution to a time step of the presented scheme in essence corresponds to finding a numerical solution to

$$\mathbf{y} \in \mathcal{N}_C(-\mathbf{z}) \quad \text{with} \quad \mathbf{R}_\mathrm{s}(\mathbf{y}, \mathbf{z}) = 0, \tag{18}$$

where $\mathbf{R}_\mathrm{s} : \mathbb{R}^n \times \mathbb{R}^n \to \mathbb{R}^n$ is an implicit relationship between $\mathbf{y}$ and $\mathbf{z}$. An extensive collection of solutions strategies for (18) can be found in Reference 20. In what follows, we limit ourselves to two strategies based on the reformulation of the normal cone inclusion as an equation including the proximal point function.

For a closed convex nonempty set $C \subseteq \mathbb{R}^n$, we define the proximal point function

$$\mathrm{prox}_C : \mathbb{R}^n \to \mathbb{R}^n, \ \mathbf{p} \mapsto \mathbf{q} = \underset{\mathbf{p}^* \in C}{\mathrm{argmin}} \left(\frac{1}{2} \|\mathbf{p} - \mathbf{p}^*\|^2 \right), \tag{19}$$

which maps a point $\mathbf{p}$ to the closest point $\mathbf{q} \in C$, where the distance between the points is measured by the Euclidean norm $\|\,.\,\|$. It is immediately clear from (19) that $\mathrm{prox}_C(\mathbf{p}) = \mathbf{p}$ if and only if $\mathbf{p} \in C$. Using the just defined proximal point function, it can be shown that two points $\mathbf{x}$ and $\mathbf{y}$ fulfill the normal cone inclusion

$$\mathbf{y} \in \mathcal{N}_C(\mathbf{x}), \tag{20}$$

if and only if they fulfill the equation

$$\mathbf{x} = \mathrm{prox}_C(\mathbf{x} + r\mathbf{y}) \tag{21}$$

for any $r > 0$, see Reference 22.

Using the equivalence of (20) and (21) allows to reformulate (18) as

$$\mathbf{z} = -\mathrm{prox}_C(r\mathbf{y} - \mathbf{z}) \quad \text{with} \quad \mathbf{R}_\mathrm{s}(\mathbf{y}, \mathbf{z}) = 0, \tag{22}$$

which reduces the problem of finding the solution of (18) to numerically finding the solution of a nonlinear equation.

Equation (22) can for example be used to define a residual $\mathbf{R} = (\mathbf{R}_\mathrm{s}^\mathrm{T} \ \mathbf{R}_\mathrm{c}^\mathrm{T})^\mathrm{T}$, where

$$\mathbf{R}_\mathrm{c}(\mathbf{x}) := \mathbf{z} + \mathrm{prox}_C(r\mathbf{y} - \mathbf{z}) = 0 \tag{23}$$

with $\mathbf{x} = (\mathbf{y}^{\mathrm{T}}\ \mathbf{z}^{\mathrm{T}})^{\mathrm{T}}$. Due to the presence of prox_C, the residual $\mathbf{R}$ is continuous but nonsmooth, hence (23) can be solved using the semismooth (nonsmooth) Newton method,[20,23] where in the Newton update

$$\mathbf{x}^{\nu+1} = \mathbf{x}^{\nu} - \nabla\mathbf{R}(\mathbf{x}^{\nu})^{-1}\mathbf{R}(\mathbf{x}^{\nu}) \tag{24}$$

any regular element $\nabla\mathbf{R}(\mathbf{x}^{\nu})$ of the generalized Jacobian $\partial\mathbf{R}(\mathbf{x}^{\nu})$ can be used. The semismooth Newton method reduces to the Newton method whenever $\mathbf{R}$ is differentiable. In that case, $\nabla\mathbf{R}(\mathbf{x}^{\nu})$ is the Jacobian matrix of $\mathbf{R}$ at $\mathbf{x}^{\nu}$.

Solving (23) with the semismooth Newton method has two drawbacks if $\nabla\mathbf{R}(\mathbf{x}^{\nu})$ is computed by finite differences. Firstly, the accuracy of the Jacobian strongly depends on the parameter r. Moreover, using finite differences to compute $\nabla\mathbf{R}(\mathbf{x}^{\nu})$ at a point where $\mathbf{R}$ is not differentiable generally leads to an arbitrary element in $\partial\mathbf{R}(\mathbf{x}^{\nu})$. Hence, we have no control over which element of $\partial\mathbf{R}(\mathbf{x}^{\nu})$ is ultimately used for the Newton update.

As a remedy, we can use an active set formulation to treat (23), which relies on the specific knowledge of the set C. In our case, two sets are of interest. Either $C = \mathbb{R}_0^- := \{z \in \mathbb{R} \mid z \leq 0\ \}$ or $C = B(R) := \{\mathbf{z} \in \mathbb{R}^n \mid \|\mathbf{z}\| \leq R\}$, for which the respective proximal point functions are piecewise given as

$$\begin{cases} p \in \mathbb{R}_0^- : & \mathrm{prox}_{\mathbb{R}_0^-}(p) = p \\ p \notin \mathbb{R}_0^- : & \mathrm{prox}_{\mathbb{R}_0^-}(p) = 0 \end{cases} \quad \text{and} \quad \begin{cases} \mathbf{p} \in B(R) : & \mathrm{prox}_{B(R)}(\mathbf{p}) = \mathbf{p} \\ \mathbf{p} \notin B(R) : & \mathrm{prox}_{B(R)}(\mathbf{p}) = R\frac{\mathbf{p}}{\|\mathbf{p}\|}. \end{cases} \tag{25}$$

It follows immediately from using (25) in (23) that for $C = \mathbb{R}_0^-$ the residual in (23) is equivalent to

$$\begin{aligned} ry - z \in \mathbb{R}_0^- : &\quad R_{\mathrm{c}} := y = 0 \\ ry - z \notin \mathbb{R}_0^- : &\quad R_{\mathrm{c}} := z = 0, \end{aligned} \tag{26}$$

where we abstain from the bold notation as all variables are scalar. Proceeding all the same for $C = B(R)$, the residual in (23) is equivalent to

$$\begin{aligned} r\mathbf{y} - \mathbf{z} \in B(R) : &\quad \mathbf{R}_{\mathrm{c}} := \mathbf{y} = 0 \\ r\mathbf{y} - \mathbf{z} \notin B(R) : &\quad \mathbf{R}_{\mathrm{c}} := \mathbf{z} + R\frac{\mathbf{y}}{\|\mathbf{y}\|} = 0, \end{aligned} \tag{27}$$

where we have used that $\mathbf{z} + R\frac{r\mathbf{y}-\mathbf{z}}{\|r\mathbf{y}-\mathbf{z}\|} = 0$ is solved by $\mathbf{z} = -R\frac{\mathbf{y}}{\|\mathbf{y}\|}$. Furthermore, $r\mathbf{y} - \mathbf{z} \notin B(R)$ implies with $\mathbf{z} \in B(R)$ that $\|\mathbf{y}\| > 0$. In these active set formulations of (23) the parameter r is only present in the activation condition of the residuals and does not affect the accuracy of the computation of the Jacobian by finite differences. Moreover, since the active set formulation gives direct access to the nondifferentiable points of the residual, we can choose to not switch between the two pieces of the residual during the numerical differentiation process, which leads to a well-behaved Jacobian and a more robust scheme.

Another popular strategy to solve (22) is the use of fixed point iterations, see References 6,23. For that, we use the implicit function theorem on $\mathbf{R}_{\mathrm{s}}(\mathbf{y}, \mathbf{z}) = 0$ guaranteeing the existence of a function $\mathbf{F}$ such that $\mathbf{y} = \mathbf{F}(\mathbf{z})$. Hence, the fixed point iterations follow as

$$\mathbf{z}^{\nu+1} = -\mathrm{prox}_C(r\mathbf{F}(\mathbf{z}^{\nu}) - \mathbf{z}^{\nu}), \tag{28}$$

where generally $\mathbf{F}$ is not known analytically and $\mathbf{y}^{\nu} = \mathbf{F}(\mathbf{z}^{\nu})$ must be found numerically by solving $\mathbf{R}_{\mathrm{s}}(\mathbf{y}^{\nu}, \mathbf{z}^{\nu}) = 0$ for $\mathbf{y}^{\nu}$ while treating $\mathbf{z}^{\nu}$ as a constant.

3 | MECHANICAL SYSTEMS WITH FRICTIONAL CONTACTS

Consider a finite-dimensional mechanical system whose motion is described by the generalized coordinates $\mathbf{q}(t) \in \mathbb{R}^n$ which are considered to be functions of time t. We introduce the generalized velocities $\mathbf{u}$ corresponding to the time derivative $\dot{\mathbf{q}}$ of the generalized coordinates for almost all t, that is, $\dot{\mathbf{q}} = \mathbf{u}$ for almost all t. Equivalently, we can write

$$\mathrm{d}\mathbf{q} = \mathbf{u}\ \mathrm{d}t. \tag{29}$$

We assume the generalized velocities to be special functions of locally bounded variation, that is, functions of locally bounded variations with no singular part, see References 24,25. This implies that the left and right limits of $\mathbf{u}$, respectively denoted as $\mathbf{u}^-$ and $\mathbf{u}^+$, exist and are bounded at every time instant, and that the discontinuity points of $\mathbf{u}$ are countable. In order to have the notion of velocity for every time instant, we set $\mathbf{u} = \mathbf{u}^+$, that is, we consider the velocities to be right continuous. It is well known, see References 2,26, that the differential measure $\mathrm{d}\mathbf{u}$ can be decomposed into the sum of an absolutely continuous measure and a singular measure with respect to the Lebesgue measure $\mathrm{d}t$. To state the decomposition, we define the atomic measure η as a finite sum of Dirac point measures δ_{t_k}. Specifically,

$$\mathrm{d}\eta = \sum_k \mathrm{d}\delta_{t_k}, \quad \text{where} \quad \int_I \mathrm{d}\delta_{t_k} = \begin{cases} 1 & \text{if } t_k \in I \\ 0 & \text{if } t_k \notin I \end{cases}. \tag{30}$$

With that, the velocity measure can be decomposed as

$$\mathrm{d}\mathbf{u} = \mathbf{a}\, \mathrm{d}t + (\mathbf{u}^+ - \mathbf{u}^-)\, \mathrm{d}\eta, \tag{31}$$

where we call the density $\mathbf{a}$ the generalized acceleration of the mechanical system and where $\mathrm{d}\eta$ is concentrated on the set of discontinuities t_k of $\mathbf{u}$. To complete the description of the dynamics of the mechanical system, the link between the change in velocity $\mathrm{d}\mathbf{u}$ and the forces acting on the system is established by the equality of measures

$$\mathbf{M}(t, \mathbf{q})\, \mathrm{d}\mathbf{u} = \mathrm{d}\mathbf{F}, \tag{32}$$

where $\mathbf{M} = \mathbf{M}^{\mathrm{T}}$ denotes the mass matrix of the system and the forces are represented by the force measure $\mathrm{d}\mathbf{F}$.

We assume that the mechanical system is subjected to $n_g + n_\gamma$ ideal bilateral constraints formulated at position and velocity level, respectively, as

$$\mathbf{g}(t, \mathbf{q}) = 0 \in \mathbb{R}^{n_g} \quad \text{and} \quad \boldsymbol{\gamma}(t, \mathbf{q}, \mathbf{u}) = 0 \in \mathbb{R}^{n_\gamma}. \tag{33}$$

By ideality of the constraint forces,[2] the corresponding force directions are given by

$$\mathbf{W}_g^{\mathrm{T}} = \frac{\partial \mathbf{g}}{\partial \mathbf{q}} \quad \text{and} \quad \mathbf{W}_\gamma^{\mathrm{T}} = \frac{\partial \boldsymbol{\gamma}}{\partial \mathbf{u}}, \tag{34}$$

such that the constraint forces are

$$\mathrm{d}\mathbf{F}_{g\gamma} = \mathbf{W}_g \mathrm{d}\mathbf{P}_g + \mathbf{W}_\gamma \mathrm{d}\mathbf{P}_\gamma, \tag{35}$$

where $\mathrm{d}\mathbf{P}_g$ and $\mathrm{d}\mathbf{P}_\gamma$ denote the constraint percussion measures. Assuming that percussions $\mathbf{P}_\square$ are special functions of locally bounded variation, the force measures $\mathrm{d}\mathbf{P}_\square$ are composed by a nonimpulsive force $\lambda_\square$ and an impulsive force $\boldsymbol{\Lambda}_\square$, that is,

$$\mathrm{d}\mathbf{P}_\square = \lambda_\square \mathrm{d}t + \boldsymbol{\Lambda}_\square \mathrm{d}\eta. \tag{36}$$

Hereby the box $\square$ is used as a placeholder for any subscript, for example, for g or γ.

To model the contacts occurring in the mechanical system, we assume that they can be described by n_N ideal unilateral constraints at position level

$$\mathbf{g}_N(t, \mathbf{q}) \geq 0, \tag{37}$$

where the inequality holds componentwise and $\mathbf{g}_N(t, \mathbf{q}) \in \mathbb{R}^{n_N}$ are the gap functions describing the distance between the tangent planes of the pairs of contact points on either contacting bodies, see References 2,27. The corresponding constraint forces are

$$\mathrm{d}\mathbf{F}_N = \mathbf{W}_N \mathrm{d}\mathbf{P}_N \quad \text{with} \quad \mathbf{W}_N^{\mathrm{T}} = \frac{\partial \mathbf{g}_N}{\partial \mathbf{q}}. \tag{38}$$

For the contact (pair) k we say that the contact is

- *open* if $g_N^k > 0$, that is, the contacting bodies are separated
- *closed* if $g_N^k = 0$, that is, the contacting bodies are in contact
- *penetrating* if $g_N^k < 0$, that is, the contacting bodies penetrate each other.

We define the set of active contacts as

$$A(t, \mathbf{q}) = \left\{ k = 1, \ \dots \ , n_N \ \middle| \ g_N^k(t, \mathbf{q}) \leq 0 \right\}. \tag{39}$$

It is clear from this definition, that the set of inactive contacts, that is, the complement $\bar{A} = \{1, \ \dots \ , n_N\} \setminus A$ of the set A, is the set of open contacts.

The constraint force laws describing a contact in normal direction are formulated separately for the nonimpulsive forces $\boldsymbol{\lambda}_N$ and the impulsive forces $\boldsymbol{\Lambda}_N$ composing the normal contact percussions $\mathrm{d}\mathbf{P}_N$ by (36). For the nonimpulsive contact force λ_N^k of the kth contact we choose Signorini's law

$$g_N^k \in \mathcal{N}_{\mathbb{R}_0^-}(-\lambda_N^k), \tag{40}$$

which assures contact impenetrability and is also known as the Signorini condition. Hereby, we assume that the contact surfaces can only exert compressive normal contact forces λ_N^k on each other. The physical interpretation of Signorini's law is easiest understood by looking at (40) as an inequality complementarity condition

$$\lambda_N^k \geq 0, \quad g_N^k \geq 0, \quad \lambda_N^k \, g_N^k = 0. \tag{41}$$

Indeed, if $\lambda_N^k > 0$, the argument of the normal cone is an interior point of the set $\mathbb{R}_0^-$ and the normal cone is zero, implying $g_N^k = 0$. On the other hand, if $\lambda_N^k = 0$, it follows from the definition of the normal cone (6) that $\mathcal{N}_{\mathbb{R}_0^-}(0)$ is the set of positive numbers including zero and therefore $g_N^k \geq 0$. It is easy to see from Signorini's law in the form (41) that for open contacts, the normal contact force is zero and if the contact is closed, only forces are allowed which push the contact surfaces apart.

For the impulsive contact forces $\boldsymbol{\Lambda}_N$, we use the gap velocity defined by

$$\dot{\boldsymbol{g}}_N(t, \mathbf{q}, \mathbf{u}) = \mathbf{W}_N^{\mathrm{T}}(t, \mathbf{q}) \ \mathbf{u} + \frac{\partial \boldsymbol{g}_N}{\partial t}(t, \mathbf{q}) \tag{42}$$

to formulate the Newton-type impact law as

$$\begin{aligned} k \in A: \quad & \xi_N^k \in \mathcal{N}_{\mathbb{R}_0^-}(-\Lambda_N^k) \\ k \in \bar{A}: \quad & \Lambda_N^k = 0. \end{aligned}$$

Herein, we have introduced the kinematic quantity

$$\xi_N^k(t, \mathbf{q}, \mathbf{u}^-, \mathbf{u}^+) = \dot{g}_N^k(t, \mathbf{q}, \mathbf{u}^+) + e_N^k \ \dot{g}_N^k(t, \mathbf{q}, \mathbf{u}^-) \tag{44}$$

for the k-th contact with restitution coefficient e_N^k. The impact law (43) implies that whenever an impact takes place, that is, $\Lambda_N^k > 0$, the postimpact velocity $\dot{g}_N^{k+} = \dot{g}_N^k(t, \mathbf{q}, \mathbf{u}^+)$ is related to the similarly defined preimpact velocity by Newton's impact law

$$\dot{g}_N^{k+} = -e_N^k \ \dot{g}_N^{k-}. \tag{45}$$

More details on the intricacies of the generalized Newton's impact law (43) can be found in References 28,29. Friction between the surfaces of the k-th contact is described by a set-valued force law. Therefore, n_F^k velocity parameters $\boldsymbol{\gamma}_F^k(t, \mathbf{q}, \mathbf{u}) \in \mathbb{R}^{n_F^k}$ describing the relative motion of the surfaces are typically introduced, where $n_F^k = 1$ for planar friction,

$n_F^k = 2$ for spatial friction and $n_F^k \geq 3$ for combined friction laws such as Coulomb–Contensou friction.[30] The friction forces have the form

$$\mathrm{d}\mathbf{F}_F = \mathbf{W}_F \mathrm{d}\mathbf{P}_F = \sum_{k=1}^{n_N} \mathbf{W}_F^k \mathrm{d}\mathbf{P}_F^k \quad \text{with} \quad (\mathbf{W}_F^k)^{\mathrm{T}} = \frac{\partial \boldsymbol{\gamma}_F^k}{\partial \mathbf{u}}, \tag{46}$$

where $\mathbf{W}_F = (\mathbf{W}_F^1 \ \dots \ \mathbf{W}_F^{n_N})$ and $\mathrm{d}\mathbf{P}_F = \left((\mathrm{d}\mathbf{P}_F^1)^{\mathrm{T}} \ \dots \ (\mathrm{d}\mathbf{P}_F^{n_N})^{\mathrm{T}}\right)^{\mathrm{T}}$.

With C_F denoting the set of admissible (negative) friction forces, the constitutive laws for the nonimpulsive and impulsive friction forces of the k-th contact are

$$\boldsymbol{\gamma}_F^k \in \mathcal{N}_{C_F(\lambda_N^k)}(-\boldsymbol{\lambda}_F^k) \quad \text{and} \quad \boldsymbol{\xi}_F^k \in \mathcal{N}_{C_F(\Lambda_N^k)}(-\boldsymbol{\Lambda}_F^k) \tag{47}$$

whenever the contact k is active, that is, $k \in A$. Moreover, the set C_F depends on the normal contact forces and we have introduced

$$\boldsymbol{\xi}_F^k(t, \mathbf{q}, \mathbf{u}^-, \mathbf{u}^+) = \boldsymbol{\gamma}_F^k(t, \mathbf{q}, \mathbf{u}^+) + e_F^k \, \boldsymbol{\gamma}_F^k(t, \mathbf{q}, \mathbf{u}^-) \tag{48}$$

with restitution coefficient e_F^k. Otherwise, if the contact k is open, the friction forces are zero.

For the sake of simplicity, in this article we restrict ourselves to sets of admissible (negative) friction forces having the form

$$C_F(\lambda_N^k) = \left\{ \lambda_F^k \in \mathbb{R}^{n_F^k} \;\middle|\; \|\lambda_F^k\| \leq \mu^k \lambda_N^k \right\} \tag{49}$$

with friction coefficient μ^k and mention how the general case can be treated wherever it seems appropriate.

The most prominent example having the form (49) is isotropic spatial Coulomb friction. As described in Reference 27, in that case we have $n_F^k = 2$ since the velocity parameters correspond to two orthogonal velocities which are tangent to the contact surfaces.

Under the premise that all forces which are not constraint or contact forces, such as spring forces, gyroscopic terms, and dashpot forces, are nonimpulsive and can therefore be represented by a Lebesgue-density $\mathbf{h}(t, \mathbf{q}, \mathbf{u})$, the totality of forces acting on the mechanical system is represented by

$$\begin{aligned} \mathrm{d}\mathbf{F} &= \mathbf{h}\mathrm{d}t + \mathrm{d}\mathbf{F}_{g\gamma} + \mathrm{d}\mathbf{F}_N + \mathrm{d}\mathbf{F}_F \\ &= \mathbf{h}\mathrm{d}t + \mathbf{W}_g \mathrm{d}\mathbf{P}_g + \mathbf{W}_\gamma \mathrm{d}\mathbf{P}_\gamma + \mathbf{W}_N \mathrm{d}\mathbf{P}_N + \mathbf{W}_F \mathrm{d}\mathbf{P}_F. \end{aligned} \tag{50}$$

Consequently, the equality of measure (32) takes the form

$$\mathbf{M}\mathrm{d}\mathbf{u} = \mathbf{h}\mathrm{d}t + \mathbf{W}_g \mathrm{d}\mathbf{P}_g + \mathbf{W}_\gamma \mathrm{d}\mathbf{P}_\gamma + \mathbf{W}_N \mathrm{d}\mathbf{P}_N + \mathbf{W}_F \mathrm{d}\mathbf{P}_F. \tag{51}$$

With (31) and (36) in mind, we conclude from (51) that the acceleration of the system is characterized by the equations of motion

$$\mathbf{M}\mathbf{a} = \mathbf{h} + \mathbf{W}_g \lambda_g + \mathbf{W}_\gamma \lambda_\gamma + \mathbf{W}_N \lambda_N + \mathbf{W}_F \lambda_F \tag{52}$$

holding for $\mathrm{d}t$-almost everywhere in time and the velocity jumps are given by the impact equations

$$\mathbf{M}(\mathbf{u}^+ - \mathbf{u}^-) = \mathbf{W}_g \Lambda_g + \mathbf{W}_\gamma \Lambda_\gamma + \mathbf{W}_N \Lambda_N + \mathbf{W}_F \Lambda_F. \tag{53}$$

4 | ACCELERATION LEVEL CONSTRAINTS AND STABILIZATION

In this section, we formulate the bilateral constraints as well as Signorini's law on acceleration level. Moreover, a stabilization on velocity and position level in the sense of Gear–Gupta–Leimkuhler is introduced to avoid constraint drift in the numerical scheme.

In order to formulate the bilateral constraints (33) on acceleration level, we introduce the constraint velocity

$$\dot{\boldsymbol{g}}(t, \mathbf{q}, \mathbf{u}) = \mathbf{W}_g^{\mathrm{T}}(t, \mathbf{q})\mathbf{u} + \frac{\partial \boldsymbol{g}}{\partial t}(t, \mathbf{q}) \tag{54}$$

as well as the constraint accelerations

$$\begin{aligned} \ddot{\boldsymbol{g}}(t, \mathbf{q}, \mathbf{u}, \mathbf{a}) &= \mathbf{W}_g^{\mathrm{T}}(t, \mathbf{q})\ \mathbf{a} + \tfrac{\partial \dot{\boldsymbol{g}}}{\partial \mathbf{q}}(t, \mathbf{q}, \mathbf{u})\ \mathbf{u} + \tfrac{\partial \dot{\boldsymbol{g}}}{\partial t}(t, \mathbf{q}, \mathbf{u}), \\ \dot{\boldsymbol{\gamma}}(t, \mathbf{q}, \mathbf{u}, \mathbf{a}) &= \mathbf{W}_\gamma^{\mathrm{T}}(t, \mathbf{q})\ \mathbf{a} + \tfrac{\partial \boldsymbol{\gamma}}{\partial \mathbf{q}}(t, \mathbf{q}, \mathbf{u})\ \mathbf{u} + \tfrac{\partial \boldsymbol{\gamma}}{\partial t}(t, \mathbf{q}, \mathbf{u}). \end{aligned} \tag{55}$$

With those, the bilateral constraints (33) are equivalently formulated by demanding

$$\ddot{\boldsymbol{g}}(t, \mathbf{q}, \mathbf{u}, \mathbf{a}) = 0 \quad \text{and} \quad \dot{\boldsymbol{\gamma}}(t, \mathbf{q}, \mathbf{u}, \mathbf{a}) = 0 \tag{56}$$

for dt-almost everywhere as well as

$$\dot{\boldsymbol{g}}(t, \mathbf{q}, \mathbf{u}^+) = 0 \quad \text{and} \quad \boldsymbol{\gamma}(t, \mathbf{q}, \mathbf{u}^+) = 0 \tag{57}$$

whenever a velocity jump occurs. Clearly, these conditions are equivalent to the original constraints only if the initial conditions are chosen appropriately, that is, the initial conditions must fulfill the original constraints (33).

As described in [2, p. 138], we can use the gap velocity (42) and the gap acceleration

$$\ddot{\boldsymbol{g}}_N(t, \mathbf{q}, \mathbf{u}, \mathbf{a}) = \mathbf{W}_N^{\mathrm{T}}(t, \mathbf{q})\ \mathbf{a} + \frac{\partial \dot{\boldsymbol{g}}_N}{\partial \mathbf{q}}(t, \mathbf{q}, \mathbf{u})\ \mathbf{u} + \frac{\partial \dot{\boldsymbol{g}}_N}{\partial t}(t, \mathbf{q}, \mathbf{u}) \tag{58}$$

to formulate the Signorini condition (40) at velocity and acceleration level, respectively. Specifically, on velocity level Signorini's law reads as

$$\begin{aligned} k \in A: &\quad \dot{g}_N^k \in \mathcal{N}_{\mathbb{R}_0^-}(-\lambda_N^k) \\ k \in \bar{A}: &\quad \lambda_N^k = 0 \end{aligned} \quad \mathrm{d}t\text{-a.e.}, \tag{59}$$

whereas on acceleration level we have

$$\begin{aligned} k \in B: &\quad \ddot{g}_N^k \in \mathcal{N}_{\mathbb{R}_0^-}(-\lambda_N^k) \\ k \in \overline{B}: &\quad \lambda_N^k = 0 \end{aligned} \quad \mathrm{d}t\text{-a.e.}, \tag{60}$$

where we have introduced the set

$$B(t, \mathbf{q}, \mathbf{u}) = \left\{ k \in A \;\middle|\; \dot{g}_N^k(t, \mathbf{q}, \mathbf{u}) \leq 0 \right\} \tag{61}$$

characterizing the contacts that are active on position as well as on velocity level. The complement of B is again denoted as $\overline{B} = \{1, \ldots, n_N\} \setminus B$ and by definition includes $\bar{A}$ as a subset, that is, $\bar{A} \subseteq \overline{B}$. It is important to point out that if the motion fulfills Signorini's law on one kinematic level, it does so also on all other kinematic levels provided that the initial conditions are compatible with the other kinematic levels.

It is well known that the constraints of a mechanical system can be formulated on acceleration level dt-almost everywhere without changing its motions. Moreover, the acceleration level constraints come with favorable mathematical properties. During impact free time intervals, for example, the presence of position level constraints leads to a DAE of index three. A formulation of the system with constraints on acceleration level reduces to a DAE of index one, which are often easier to solve numerically than higher index DAEs. However, the described index reduction by differentiation is prone to numerical drift, meaning that although the constraint is satisfied on acceleration level, the corresponding position and velocity level constraints are violated due to numerical integration errors. As a remedy, the position and velocity level constraints can be stabilized by introducing additional Lagrange multipliers. This stabilization, initially proposed

by Reference 8 and hence known by the name Gear–Gupta–Leimkuhler (GGL) method, can analogously be extended to unilateral constraints, see Reference 13.

To stabilize the constraints, we formally extend the kinematics of the system to

$$\begin{aligned} \mathrm{d}\mathbf{q} &= (\mathbf{u} + \mathbf{u}_S)\,\mathrm{d}t, \\ \mathrm{d}\mathbf{u} &= (\mathbf{a} + \mathbf{a}_S)\,\mathrm{d}t + (\mathbf{u}^+ - \mathbf{u}^-)\,\mathrm{d}\eta, \end{aligned} \tag{62}$$

where we have added the velocity $\mathbf{u}_S$ and the acceleration $\mathbf{a}_S$ caused by the stabilization to (29) and (31), respectively. The multipliers $\boldsymbol{\nu}_g$, $\boldsymbol{\nu}_\gamma$, and $\boldsymbol{\nu}_N$ then take care of the stabilization of (56) and (60) on velocity level by demanding

$$\begin{aligned} \mathbf{M}\mathbf{a}_S &= \mathbf{W}_g\boldsymbol{\nu}_g + \mathbf{W}_\gamma\boldsymbol{\nu}_\gamma + \mathbf{W}_N\boldsymbol{\nu}_N \\ \dot{\boldsymbol{g}}(t,\mathbf{q},\mathbf{u}) &= 0 \quad \mathrm{d}t\text{-a.e.} \\ \boldsymbol{\gamma}(t,\mathbf{q},\mathbf{u}) &= 0 \quad \mathrm{d}t\text{-a.e.} \\ k \in A: \quad \dot{g}_N^k &\in \mathcal{N}_{\mathbb{R}_0^-}(-\nu_N^k) \quad \mathrm{d}t\text{-a.e.} \\ k \in \bar{A}: \quad \nu_N^k &= 0. \end{aligned} \tag{63}$$

Note, that the stabilization (63) demands $\dot{\boldsymbol{g}} = 0$ for almost all time instants, which combined to (57) yields the condition $\dot{\boldsymbol{g}} = 0$ for all time instants. The same reasoning holds for $\boldsymbol{\gamma} = 0$.

We use the multipliers $\boldsymbol{\mu}_g$ and $\boldsymbol{\mu}_N$ to stabilize the constraints (56) and (60) on position level by

$$\begin{aligned} \mathbf{M}\mathbf{u}_S &= \mathbf{W}_g\boldsymbol{\mu}_g + \mathbf{W}_N\boldsymbol{\mu}_N, \\ \boldsymbol{g}(t,\mathbf{q}) &= 0, \\ g_N^k &\in \mathcal{N}_{\mathbb{R}_0^-}(-\mu_N^k) \end{aligned} \tag{64}$$

for all contacts k.

It can be shown that, in absence of numerical errors, the solution of the equations of motion formulated with stabilized acceleration level constraints have vanishing Lagrange multipliers $\boldsymbol{\nu}_\square$ and $\boldsymbol{\mu}_\square$ $\mathrm{d}t$-almost everywhere and therefore $\mathbf{a}_S = \mathbf{u}_S = 0$ for almost all time instants. Moreover, it can be shown that the remaining quantities solve the equations of motion with constraints formulated on position and velocity level described in Section 3. This fact establishes the mechanical equivalence of the original equations of motion of Section 3 and the equations of motion with stabilized acceleration level constraints presented in this section.

5 | NONSMOOTH GENERALIZED-α DISCRETIZATION

To compute the motion of the mechanical system numerically, in this section we derive a time-stepping scheme from the family of generalized-α methods. The scheme is derived by integrating the equations of motion with stabilized acceleration level constraints over a time interval $I = (t_i, t_{i+1}]$ and introducing appropriate discrete variables.

Considering the velocity $\mathbf{u}(t)$ as a right-continuous function, the velocity of the system at a time t can be written as

$$\mathbf{u}(t) = \mathbf{u}(t_i) + \int_{(t_i,t]} \mathrm{d}\mathbf{u} = \mathbf{u}(t_i) + \int_{t_i}^{t} \mathbf{a}\,\mathrm{d}t + \int_{(t_i,t]} (\mathbf{a}_S\,\mathrm{d}t + (\mathbf{u}^+ - \mathbf{u}^-)\,\mathrm{d}\eta), \tag{65}$$

where we have used (62). Similarly, the position of the system at time t_{i+1} is

$$\mathbf{q}(t_{i+1}) = \mathbf{q}(t_i) + \int_I \mathrm{d}\mathbf{q} = \mathbf{q}(t_i) + \int_I \mathbf{u}\,\mathrm{d}t + \int_I \mathbf{u}_S\,\mathrm{d}t, \tag{66}$$

which with the help of (65) can be reformulated to

$$\mathbf{q}(t_{i+1}) = \mathbf{q}(t_i) + \int_I \mathbf{u}(t_i)\,\mathrm{d}t + \int_I \int_{t_i}^{t} \mathbf{a}\,\mathrm{d}\tau\,\mathrm{d}t + \int_I \mathbf{U}(t,t_i)\,\mathrm{d}t + \int_I \mathbf{u}_S\,\mathrm{d}t, \tag{67}$$

where we have denoted the last integral in (65) by

$$\mathbf{U}(t, t_i) = \int_{(t_i,t]} (\mathbf{a}_S \, \mathrm{d}t + (\mathbf{u}^+ - \mathbf{u}^-) \, \mathrm{d}\eta). \tag{68}$$

To derive the position and velocity updates of the scheme, numerical approximations of the integrals in (65) and (67) using quadratures have to be introduced. As approximants for the position, velocity, and acceleration at some time instant t_i we introduce $\mathbf{q}_i$, $\mathbf{u}_i$, and $\mathbf{a}_i$, respectively. Moreover, we define the discrete variables

$$\mathbf{U}_{i+1} = \mathbf{U}(t_{i+1}, t_i) \quad \text{and} \quad \mathbf{Q}_{i+1} = \int_I \mathbf{U}(t, t_i) \, \mathrm{d}t + \int_I \mathbf{u}_S \, \mathrm{d}t. \tag{69}$$

The integrals of the acceleration $\mathbf{a}$ in (65) and (67) are discretized in the fashion of a generalized-α method[13] using the quadratures

$$\begin{aligned} \int_I \mathbf{a} \, \mathrm{d}t &\approx \Delta t \left((1-\gamma)\bar{\mathbf{a}}_i + \gamma \bar{\mathbf{a}}_{i+1} \right) \\ \int_I \int_{t_i}^{t} \mathbf{a} \, \mathrm{d}\tau \, \mathrm{d}t &\approx \frac{\Delta t^2}{2} \left((1-2\beta)\bar{\mathbf{a}}_i + 2\beta \bar{\mathbf{a}}_{i+1} \right), \end{aligned} \tag{70}$$

where the auxiliary acceleration variables $\bar{\mathbf{a}}$ are linked to the approximants of the acceleration by

$$\alpha_m \bar{\mathbf{a}}_i + (1-\alpha_m)\bar{\mathbf{a}}_{i+1} = \alpha_f \mathbf{a}_i + (1-\alpha_f)\mathbf{a}_{i+1} \tag{71}$$

and the time step of the scheme is introduced as $\Delta t = t_{i+1} - t_i$. The coefficients α_f, α_m, β, and γ can be chosen according to Newmark,[31] Hilber–Hughes–Taylor,[15] or Chung and Hulbert.[16] We choose the last option, which results in a second-order scheme with an adjustable level of numerical dissipation in the high-frequency range. We introduce the spectral radius at infinite frequencies $\rho_\infty \in [0, 1]$, which controls the dissipation in the high-frequency range. The coefficients of the scheme are then given by

$$\alpha_m = \frac{2\rho_\infty - 1}{\rho_\infty + 1}, \; \alpha_f = \frac{\rho_\infty}{\rho_\infty + 1}, \; \gamma = \frac{1}{2} + \alpha_f - \alpha_m \text{ and } \beta = \frac{1}{4}\left(\frac{1}{2} + \gamma\right)^2. \tag{72}$$

For $\rho_\infty = 1$ the scheme shows the minimal and for $\rho_\infty = 0$ the maximal amount of dissipation in the high-frequency regime.

Finally, the position and velocity updates

$$\begin{aligned} \mathbf{u}_{i+1} &= \mathbf{u}_i + \Delta t \left((1-\gamma)\bar{\mathbf{a}}_i + \gamma \bar{\mathbf{a}}_{i+1} \right) + \mathbf{U}_{i+1}, \\ \mathbf{q}_{i+1} &= \mathbf{q}_i + \Delta t \, \mathbf{u}_i + \frac{\Delta t^2}{2} \left((1-2\beta)\bar{\mathbf{a}}_i + 2\beta \bar{\mathbf{a}}_{i+1} \right) + \mathbf{Q}_{i+1} \end{aligned} \tag{73}$$

are obtained by using (70) and (69) in (65) and (67), respectively.

The equations of motion (52) are discretized as

$$\mathbf{M}_{i+1} \, \mathbf{a}_{i+1} = \mathbf{h}_{i+1} + \sum_{\square \in \{g,\gamma,N,F\}} \mathbf{W}_{\square,i+1} \, \lambda_{\square,i+1}, \tag{74}$$

where the subscript $i+1$ indicates that the quantity is evaluated at t_{i+1}, $\mathbf{q}_{i+1}$ and when applicable at $\mathbf{u}_{i+1}$, for example, $\mathbf{h}_{i+1} = \mathbf{h}(t_{i+1}, \mathbf{q}_{i+1}, \mathbf{u}_{i+1})$ and $\mathbf{M}_{i+1} = \mathbf{M}(t_{i+1}, \mathbf{q}_{i+1})$. Moreover, we have introduced $\lambda_{\square,i+1}$ to approximate the forces $\lambda_\square$.

To find the discrete equations for $\mathbf{U}_{i+1}$, consider the approximation

$$\int_I \mathbf{M}(\mathbf{a}_S \, \mathrm{d}t + (\mathbf{u}^+ - \mathbf{u}^-) \, \mathrm{d}\eta) \approx \mathbf{M}_{i+1}\mathbf{U}_{i+1}, \tag{75}$$

which is exact for a constant mass matrix. Furthermore, we approximate

$$\int_I \mathbf{W}_K(\boldsymbol{\nu}_K \mathrm{d}t + \boldsymbol{\Lambda}_K \mathrm{d}\eta) \approx \mathbf{W}_{K,i+1}\boldsymbol{\Lambda}_{K,i+1} \quad \text{and} \quad \int_I \mathbf{W}_F \boldsymbol{\Lambda}_F \mathrm{d}\eta \approx \mathbf{W}_{F,i+1}\boldsymbol{\Lambda}_{F,i+1}, \tag{76}$$

which are exact if $\mathbf{W}_\square$ is constant and where we have introduced the discrete variables

$$\boldsymbol{\Lambda}_{K,i+1} := \int_I \boldsymbol{\nu}_K \mathrm{d}t + \boldsymbol{\Lambda}_K \mathrm{d}\eta \quad \text{and} \quad \boldsymbol{\Lambda}_{F,i+1} := \int_I \boldsymbol{\Lambda}_F \mathrm{d}\eta \tag{77}$$

with $K \in \{g, \gamma, N\}$. In view of (53) and (63), the above discretizations (75) and (76) yield the discrete impact equations

$$\mathbf{M}_{i+1}\mathbf{U}_{i+1} = \sum_{K\in\{g,\gamma,N\}} \mathbf{W}_{K,i+1}\boldsymbol{\Lambda}_{K,i+1} + \mathbf{W}_{F,i+1}\boldsymbol{\Lambda}_{F,i+1}. \tag{78}$$

From the definition of the atomic measure (30), we see that the discrete variables $\boldsymbol{\Lambda}_{K,i+1}$ and $\boldsymbol{\Lambda}_{F,i+1}$ consist of the sum of impulsive forces $\sum_k \boldsymbol{\Lambda}_K(t_k)$, respectively $\sum_k \boldsymbol{\Lambda}_F(t_k)$, corresponding to collisions in the time interval I. In addition, $\boldsymbol{\Lambda}_{K,i+1}$ contains a contribution due to the stabilization of the constraints.

The discrete equation for $\mathbf{Q}_{i+1}$ is found from the approximation

$$\int_I \int_{(t_i,t]} \mathbf{M}(\mathbf{a}_S \, \mathrm{d}\tau + (\mathbf{u}^+ - \mathbf{u}^-) \, \mathrm{d}\eta)\mathrm{d}t + \int_I \mathbf{M}\mathbf{u}_S \mathrm{d}t \approx \mathbf{M}_{i+1}\mathbf{Q}_{i+1}. \tag{79}$$

Finally, it is by combining the impact equation (53) with the stabilizing conditions (63) and (64) that we can motivate the discrete equation

$$\mathbf{M}_{i+1}\mathbf{Q}_{i+1} = \sum_{K\in\{g,N\}} \mathbf{W}_{K,i+1}\boldsymbol{\kappa}_{K,i+1} + \sum_{R\in\{\gamma,F\}} \frac{\Delta t}{2}\mathbf{W}_{R,i+1}\boldsymbol{\Lambda}_{R,i+1}. \tag{80}$$

Hereby, we have introduced the discrete variables $\boldsymbol{\kappa}_{K,i+1}$ with $K \in \{g, N\}$ as

$$\boldsymbol{\kappa}_{K,i+1} := \int_I \int_{(t_i,t]} (\boldsymbol{\nu}_K \mathrm{d}\tau + \boldsymbol{\Lambda}_K \mathrm{d}\eta)\mathrm{d}t + \int_I \boldsymbol{\mu}_K \mathrm{d}t \tag{81}$$

and have used the approximation

$$\int_I \int_{(t_i,t]} \mathbf{W}_K(\boldsymbol{\nu}_K \mathrm{d}t + \boldsymbol{\Lambda}_K \mathrm{d}\eta)\mathrm{d}t + \int_I \mathbf{W}_K \boldsymbol{\mu}_K \mathrm{d}t \approx \mathbf{W}_{K,i+1}\boldsymbol{\kappa}_{K,i+1}, \tag{82}$$

similar to (76). Moreover, we have approximated the remaining double integrals by

$$\int_I \int_{(t_i,t]} (\boldsymbol{\nu}_\gamma \mathrm{d}t + \boldsymbol{\Lambda}_\gamma \mathrm{d}\eta) \, \mathrm{d}t \approx \frac{\Delta t}{2}\boldsymbol{\Lambda}_{\gamma,i+1} \quad \text{and} \quad \int_I \int_{(t_i,t]} \boldsymbol{\Lambda}_F \mathrm{d}\eta \, \mathrm{d}t \approx \frac{\Delta t}{2}\boldsymbol{\Lambda}_{F,i+1}. \tag{83}$$

Similar to standard DAE solvers,[32] the bilateral constraints on all kinematic levels are discretized by just evaluating them at the end of the time step. For the constraints originating from a position level constraint that is

$$\boldsymbol{g}(t_{i+1}, \mathbf{q}_{i+1}) = 0, \quad \dot{\boldsymbol{g}}(t_{i+1}, \mathbf{q}_{i+1}, \mathbf{u}_{i+1}) = 0 \quad \text{and} \quad \ddot{\boldsymbol{g}}(t_{i+1}, \mathbf{q}_{i+1}, \mathbf{u}_{i+1}, \mathbf{a}_{i+1}) = 0, \tag{84}$$

whereas for constraints originating from a velocity level constraint, we have

$$\boldsymbol{\gamma}(t_{i+1}, \mathbf{q}_{i+1}, \mathbf{u}_{i+1}) = 0 \quad \text{and} \quad \dot{\boldsymbol{\gamma}}(t_{i+1}, \mathbf{q}_{i+1}, \mathbf{u}_{i+1}, \mathbf{a}_{i+1}) = 0. \tag{85}$$

6 | DISCRETE NORMAL CONTACT LAWS

Since we aim at an event-capturing time-stepping scheme, we do not resolve the contact dynamics during a time step $I = (t_i, t_{i+1}]$ in all detail, but rather derive discrete contact laws capturing the contact dynamics occurring during the time step. More precisely, we derive discrete normal contact laws such that at the end of the time step impenetrability is satisfied on all kinematic levels while capturing the effects of Newton's impact law.

We start the discretization of the normal contact laws from the acceleration level Signorini conditions (60). Since the velocity of the system is continuous between velocity jumps, implying $\dot{g}_N^{k+} = \dot{g}_N^{k-} = \dot{g}_N^k$ dt-a.e., we have that

$$(1 + e_N^k)\dot{g}_N^k = \dot{g}_N^{k+} + e_N^k \dot{g}_N^{k-} = \xi_N^k \quad \mathrm{d}t\text{-a.e.}, \tag{86}$$

where we have used the definition (44) of ξ_N^k. Consequently, in view of $e_N^k \geq 0$, we can replace the condition $\dot{g}_N^k \leq 0$ with $\xi_N^k \leq 0$ in (61). The discrete Signorini conditions then result by evaluating all quantities in (60) at the end of the time step. Thus, we have

$$\begin{aligned} k \in B_{i+1} &: \quad \ddot{g}_{N,i+1}^k \in \mathcal{N}_{\mathbb{R}_0^-}(-\lambda_{N,i+1}^k) \\ k \in \overline{B}_{i+1} &: \quad \lambda_{N,i+1}^k = 0 \end{aligned}, \tag{87}$$

where we have used the notation

$$\begin{aligned} g_{N,i+1}^k &= g_N^k(t_{i+1}, \mathbf{q}_{i+1}) \\ \xi_{N,i+1}^k &= \xi_N^k(t_{i+1}, \mathbf{q}_{i+1}, \mathbf{u}_i, \mathbf{u}_{i+1}) \\ \ddot{g}_{N,i+1}^k &= \ddot{g}_N^k(t_{i+1}, \mathbf{q}_{i+1}, \mathbf{u}_{i+1}, \mathbf{a}_{i+1}) \end{aligned} \tag{88}$$

and defined the discrete version of (61) as

$$B_{i+1} = \left\{ k \in A_{i+1} \;\middle|\; \xi_{N,i+1}^k \leq 0 \right\}, \text{ where } \quad A_{i+1} = A(t_{i+1}, \mathbf{q}_{i+1}). \tag{89}$$

To formulate the normal contact law on velocity level, we combine Signorini's law on velocity level, the impact law and the stabilization condition. For that, consider the case of active normal contact, that is, $k \in A$. Then, Signorini's law and the stabilization condition

$$\dot{g}_N^k \in \mathcal{N}_{\mathbb{R}_0^-}(-\lambda_N^k) \quad \text{and} \quad \dot{g}_N^k \in \mathcal{N}_{\mathbb{R}_0^-}(-\nu_N^k) \tag{90}$$

hold dt-almost everywhere, respectively. Using the cone property of the normal cone, we may write $(1 + e_N^k)$ in front of $\dot{g}_N^k$ in (90), which in view of (86) takes the form

$$\xi_N^k \in \mathcal{N}_{\mathbb{R}_0^-}(-\lambda_N^k) \quad \text{and} \quad \xi_N^k \in \mathcal{N}_{\mathbb{R}_0^-}(-\nu_N^k). \tag{91}$$

The proposed reformulation of the combined Signorini and stabilization condition has the same form as the impact law (43), which reads as

$$\xi_N^k \in \mathcal{N}_{\mathbb{R}_0^-}(-\Lambda_N^k). \tag{92}$$

With this preparatory work, we can finally proceed toward a discrete law. Since we are interested in the end of the time step, we use the set A_{i+1} introduced in (89) to determine whether the contact k is active on position level at the end of the time step. If this contact is active, that is, $k \in A_{i+1}$, we assume the contact to be active during the whole time step. Furthermore, we assume ξ_N^k to be constant within a time step $I = (t_i, t_{i+1}]$ and to correspond to $\xi_{N,i+1}^k$, which allows to combine (91) and (92) in integral form as

$$k \in A_{i+1} : \quad \xi_{N,i+1}^k \in \mathcal{N}_{\mathbb{R}_0^-}\left(-\int_I \left((\lambda_N^k + \nu_N^k)\mathrm{d}t + \Lambda_N^k \mathrm{d}\eta \right) \right), \tag{93}$$

where we have used Proposition 2. If $k \in \bar{A}_{i+1}$, the integral in (93) is zero.

At this point it is appropriate to qualitatively discuss the assumptions leading to (93). For that, we look at two cases. Either there is no collision in the time interval I and only nonimpulsive motion takes place on I(case i) or there is impulsive motion during the time interval I (case ii).

(i) *Purely nonimpulsive motion on I:* Since the contact is closed at the end of the time step and there is no collision, the contact must either have been closed during the whole time step, or it must have closed at some $t_c \in I = (t_i, t_{i+1}]$ with $\dot{g}_N^k(t_c) = 0$. In the first case, the contact velocity $\dot{g}_N^k$ vanishes on I and by (86) we have $\xi_N^k = 0$ on I justifying the approximation. In the second case, for which the contact closes during the time step we have $\dot{g}_N^k(t_i) < 0$ and $\dot{g}_N^k(t_{i+1}) \geq 0$, which is at best approximated by $\xi_{N,i+1}^k = 0$. This allows the integral over the contact forces in (93) to be nonzero, which can capture the exact dynamics.

(ii) *Impulsive motion on I:* There are one or more collisions or other events causing impulsive motion (a dynamic catastrophe). Then we have to admit that the impulsive part of the motion is dominating the dynamics on I and we may neglect the nonimpulsive motion. The error which we then make in the nonimpulsive description by falsely considering ξ_N^k to be constant is then small and of the order of the time step. If the collision takes place at $t_c \in I = (t_i, t_{i+1}]$, then we approximate $\xi_N^k(t_c, \mathbf{q}(t_c), \mathbf{u}^-(t_c), \mathbf{u}^+(t_c))$ by $\xi_N^k(t_{i+1}, \mathbf{q}(t_{i+1}), \mathbf{u}(t_i), \mathbf{u}(t_{i+1}))$. This approximation becomes exact in the limit of $\Delta t \downarrow 0$.

Finally, Equation (93) suggests a discrete normal contact law on velocity level given by

$$\begin{aligned} k \in A_{i+1} : \quad & \xi_{N,i+1}^k \in \mathcal{N}_{\mathbb{R}_0^-}(-P_{N,i+1}^k) \\ k \in \bar{A}_{i+1} : \quad & P_{N,i+1}^k = 0, \end{aligned} \tag{94}$$

where the discrete percussion is defined by

$$\mathbf{P}_{N,i+1} = \mathbf{\Lambda}_{N,i+1} + \Delta t \left((1-\gamma)\overline{\lambda}_{N,i} + \gamma \overline{\lambda}_{N,i+1} \right). \tag{95}$$

Hereby, we have introduced the auxiliary force variables $\overline{\lambda}_N$ linked to the approximants of the contact forces by

$$\alpha_m \overline{\lambda}_{N,i} + (1-\alpha_m)\overline{\lambda}_{N,i+1} = \alpha_f \lambda_{N,i} + (1-\alpha_f)\lambda_{N,i+1}. \tag{96}$$

To motivate (94) as an approximation of (93), we first state that the second part of the discrete percussion (95) is a generalized-α discretization of the integral of λ_N over I, see (70) and (71). This, in combination with (77), indeed shows that the discrete percussion approximates the integral appearing in (93), that is,

$$\mathbf{P}_{N,i+1} \approx \int_I ((\lambda_N + \nu_N)\mathrm{d}t + \mathbf{\Lambda}_N \mathrm{d}\eta)\, 36) = \int_I (\mathrm{d}\mathbf{P}_N + \nu_N \mathrm{d}t). \tag{97}$$

We use the terminology "percussion", even though the discrete variable includes the stabilizing Lagrange multipliers.

In order to state the contact law on position level, we observe that (93) also holds if we only integrate over a time span $(t_i, t] \subseteq I$. Moreover, the inclusion (93) implies that the integral is nonnegative if the contact k is closed at the end of the time step. Since, in addition, the integral is zero if the contact k is open at the end of the time step, it follows that

$$g_{N,i+1}^k \in \mathcal{N}_{\mathbb{R}_0^-}\left(-\int_{(t_i,t]} \left((\lambda_N^k + \nu_N^k)\mathrm{d}\tau + \Lambda_N^k \mathrm{d}\eta \right) \right) \tag{98}$$

for all $t \in I$. Moreover, we approximate the stabilization on position level (64) by

$$g_{N,i+1}^k \in \mathcal{N}_{\mathbb{R}_0^-}(-\mu_N^k(t)) \tag{99}$$

for all times t in I. Finally, we use the Proposition 2 to combine (98) and (99) to

$$g_{N,i+1}^k \in \mathcal{N}_{\mathbb{R}_0^-}\left(-\left(\int_I \int_{(t_i,t]} \left((\lambda_N^k + \nu_N^k)\mathrm{d}\tau + \Lambda_N^k \mathrm{d}\eta \right) \mathrm{d}t + \int_I \mu_N^k \mathrm{d}t \right) \right). \tag{100}$$

This inclusion suggests a discrete normal contact law on position level given by

$$g_{N,i+1}^k \in \mathcal{N}_{\mathbb{R}_0^-}(-\hat{\kappa}_{N,i+1}^k) \quad \text{with} \quad k = 1, \ldots, n_N, \tag{101}$$

together with

$$\hat{\boldsymbol{\kappa}}_{N,i+1} = \boldsymbol{\kappa}_{N,i+1} + \frac{\Delta t^2}{2}\left((1-2\beta)\overline{\boldsymbol{\lambda}}_{N,i} + 2\beta\overline{\boldsymbol{\lambda}}_{N,i+1}\right). \tag{102}$$

Hereby, the second part in (102) approximates the double integral of $\boldsymbol{\lambda}_N$ using the generalized-α method, see (70) and (71), and it therefore follows from (81) that

$$\hat{\boldsymbol{\kappa}}_{N,i+1} \approx \int_I \int_{(t_i,t]} ((\boldsymbol{\lambda}_N + \boldsymbol{\nu}_N)\mathrm{d}\tau + \boldsymbol{\Lambda}_N \mathrm{d}\eta)\,\mathrm{d}t + \int_I \boldsymbol{\mu}_N \mathrm{d}t, \tag{103}$$

which confirms that (101) is indeed an approximation of (100).

7 | DISCRETE FRICTION LAWS

In (47) we stated the friction law of the k-th contact as

$$\boldsymbol{\gamma}_F^k \in \mathcal{N}_{C_F(\lambda_N^k)}(-\boldsymbol{\lambda}_F^k) \tag{104}$$

for the case where the contact is active, that is, $k \in A$. Using the cone property of the normal cone, we may write $(1+e_F^k)$ in front of $\boldsymbol{\gamma}_F^k$ in (104). Furthermore, for almost all t it holds that $\mathbf{u}^+(t) = \mathbf{u}^-(t) = \mathbf{u}(t)$. Hence, it follows from (48) that we may equivalently write the friction law as

$$\boldsymbol{\xi}_F^k \in \mathcal{N}_{C_F(\lambda_N^k)}(-\boldsymbol{\lambda}_F^k). \tag{105}$$

This reformulation of the friction law brings it in a similar form as the frictional impact law (47)

$$\boldsymbol{\xi}_F^k \in \mathcal{N}_{C_F(\Lambda_N^k)}(-\boldsymbol{\Lambda}_F^k). \tag{106}$$

In the following discretization process, we exploit that the set of admissible (negative) friction forces has the homogeneity property $C_F(\alpha) = \alpha C_F(1)$. Moreover, similar as for the laws in normal direction, we consider $\boldsymbol{\xi}_F^k$ to be constant on the short time-interval I and assume it to take the value

$$\boldsymbol{\xi}_{F,i+1}^k = \boldsymbol{\xi}_F^k(t_{i+1}, \mathbf{q}_{i+1}, \mathbf{u}_i, \mathbf{u}_{i+1}).$$

Specifically, this translates to the friction law as

$$\boldsymbol{\xi}_{F,i+1}^k \in \mathcal{N}_{C_F(\lambda_N^k(t))}\left(-\boldsymbol{\lambda}_F^k(t)\right), \quad \forall t \in I. \tag{107}$$

Because $\boldsymbol{\xi}_{F,i+1}^k$ is constant on I, we can invoke (17), that is, Proposition 2 in integral form, which directly gives

$$\boldsymbol{\xi}_{F,i+1}^k \in \mathcal{N}_{C_F(\int_I \lambda_N^k \mathrm{d}t)}\left(-\int_I \boldsymbol{\lambda}_F^k\,\mathrm{d}t\right). \tag{108}$$

For the impulsive part of the motion on I, we similarly have the approximation

$$\boldsymbol{\xi}_{F,i+1}^k \in \mathcal{N}_{C_F(\Lambda_N^k(t))}\left(-\boldsymbol{\Lambda}_F^k(t)\right), \quad \forall t \in I \tag{109}$$

and using (17) cast the impact law in integral form

$$\boldsymbol{\xi}_{F,i+1}^k \in \mathcal{N}_{C_F(\int_I \Lambda_N^k\ \mathrm{d}\eta)}\left(-\int_I \boldsymbol{\Lambda}_F^k \mathrm{d}\eta\right). \tag{110}$$

Finally, we combine (108) and (110) by using Proposition 2 to

$$\boldsymbol{\xi}^k_{F,i+1} \in \mathcal{N}_{C_F(\int_I \lambda^k_N \mathrm{d}t + \Lambda^k_N \mathrm{d}\eta)} \left(- \int_I (\lambda^k_F \mathrm{d}t + \boldsymbol{\Lambda}^k_F \mathrm{d}\eta) \right), \tag{111}$$

which motivates as approximation the discrete friction law

$$\begin{aligned} k \in A_{i+1} \ : \quad & \boldsymbol{\xi}^k_{F,i+1} \in \mathcal{N}_{C_F(P^k_{N,i+1})}(-\mathbf{P}^k_{F,i+1}) \\ k \in \bar{A}_{i+1} \ : \quad & \mathbf{P}^k_{F,i+1} = 0, \end{aligned} \tag{112}$$

where

$$\mathbf{P}_{F,i+1} = \boldsymbol{\Lambda}_{F,i+1} + \Delta t \left((1-\gamma) \overline{\lambda}_{F,i} + \gamma \overline{\lambda}_{F,i+1} \right). \tag{113}$$

Hereby, we have introduced the auxiliary discrete friction forces linked to the actual forces by

$$\alpha_m \overline{\lambda}_{F,i} + (1-\alpha_m) \overline{\lambda}_{F,i+1} = \alpha_f \lambda_{F,i} + (1-\alpha_f) \lambda_{F,i+1}. \tag{114}$$

Clearly, because of (77) and interpreting the second part of (113) as the generalized-α approximation of the integral of the nonimpulsive friction forces, we have

$$\mathbf{P}_{F,i+1} \approx \int_I (\boldsymbol{\Lambda}_F \mathrm{d}\eta + \lambda_F \mathrm{d}t) 36) = \int_I \mathrm{d}\mathbf{P}_F. \tag{115}$$

Using the discrete percussion $P^k_{N,i+1}$ in (112) is finally justified by (97) since the stabilizing Lagrange multipliers are zero for the exact solution.

Since the discrete friction law (112) combines the effects of nonimpulsive and impulsive friction forces, an additional friction law is needed to distinguish these effects and compute values for both $\lambda^k_{F,i+1}$ and $\boldsymbol{\Lambda}^k_{F,i+1}$. For that, we first state that the friction law (112) basically consists of three cases. Either the kth contact is open ($k \in \bar{A}_{i+1}$) and $\mathbf{P}^k_{F,i+1} = 0$ or the contact is active ($k \in A_{i+1}$) and one of the following two cases holds. In the first case, the negative discrete percussion lies in the interior of the set of admissible negative friction forces $C_F(P^k_{N,i+1})$, which by the normal cone inclusion in (112) implies $\boldsymbol{\xi}^k_{F,i+1} = 0$. Hence, this can be seen as the case of sticking contact and we introduce the set of sticking contacts

$$D^{\mathrm{st}}_{i+1} = \left\{ k \in A_{i+1} \;\middle|\; \boldsymbol{\xi}^k_{F,i+1} = 0 \right\}. \tag{116}$$

The second case is the case of slipping contact, where $\boldsymbol{\xi}^k_{F,i+1}$ is nonzero and the negative discrete percussion must lie on the boundary of the set $C_F(P^k_{N,i+1})$ by (112). We write $k \in D^{\mathrm{sl}}_{i+1}$ in that case, where obviously the set of slipping contacts is just the complement of the set of sticking contacts, that is, $D^{\mathrm{sl}}_{i+1} = A_{i+1} \setminus D^{\mathrm{st}}_{i+1}$.

We are now ready to state the remaining discrete friction law as

$$\begin{aligned} k \in D^{\mathrm{st}}_{i+1} \ : \quad & \dot{\boldsymbol{\gamma}}^k_{F,i+1} \in \mathcal{N}_{C_F(\lambda^k_{N,i+1})}(-\boldsymbol{\lambda}^k_{F,i+1}) \\ k \in D^{\mathrm{sl}}_{i+1} \ : \quad & \boldsymbol{\lambda}^k_{F,i+1} = \boldsymbol{\lambda}^{k,\mathrm{sl}}_{F,i+1} \\ k \in \bar{A}_{i+1} \ : \quad & \boldsymbol{\lambda}^k_{F,i+1} = 0, \end{aligned} \tag{117}$$

where $\boldsymbol{\lambda}^{k,\mathrm{sl}}_{F,i+1}$ denotes the element on the boundary of $C_F(\lambda^k_{N,i+1})$ such that

$$\boldsymbol{\gamma}^k_{F,i+1} \in \mathcal{N}_{C_F(\lambda^k_{N,i+1})}(-\boldsymbol{\lambda}^{k,\mathrm{sl}}_{F,i+1}) \tag{118}$$

and $\dot{\boldsymbol{\gamma}}^k_{F,i+1}$ denotes the evaluation at the end of the time step of the acceleration

$$\dot{\boldsymbol{\gamma}}^k_F(t,\mathbf{q},\mathbf{u},\mathbf{a}) = (\mathbf{W}^k_F)^{\mathrm{T}}(t,\mathbf{q})\ \mathbf{a} + \frac{\partial \boldsymbol{\gamma}^k_F}{\partial \mathbf{q}}(t,\mathbf{q},\mathbf{u})\ \mathbf{u} + \frac{\partial \boldsymbol{\gamma}^k_F}{\partial t}(t,\mathbf{q},\mathbf{u}). \tag{119}$$

In our case, the set of admissible friction forces is given by (49) and one can easily verify that

$$\lambda_{F,i+1}^{k,\mathrm{sl}} = -\mu^k \lambda_{N,i+1}^k \frac{\boldsymbol{\gamma}_{F,i+1}^k}{\|\boldsymbol{\gamma}_{F,i+1}^k\|}. \tag{120}$$

In essence, the discrete friction law (117) corresponds to the evaluation of (104) at the end of the time step, with the difference that in the sticking case, the friction law is formulated on acceleration level. We refer to [2, sect. 10.4] for more details on this matter. We conclude this section with the remark, that the formulation of the sticking case on acceleration level is strictly necessary, because otherwise the two discrete friction laws would lead to an ambiguity. Specifically, in the sticking case, (112) would imply $\boldsymbol{\xi}_{F,i+1}^k = 0$ and the evaluation of (104) at the end of the time step would imply $\boldsymbol{\gamma}_{F,i+1}^k = 0$, which are the same condition in the case of $e_F^k = 0$. Hence, in that case the two conditions collapse and create an ambiguity which does not allow to compute $\lambda_{F,i+1}^k$ and $\boldsymbol{\Lambda}_{F,i+1}^k$ independently.

8 | EXTENSION TO GENERAL VELOCITIES

We generalize the kinematic equation (29) to

$$\mathrm{d}\mathbf{q} = \dot{\mathbf{q}}(t,\mathbf{q},\mathbf{u})\,\mathrm{d}t, \quad \text{where} \quad \dot{\mathbf{q}}(t,\mathbf{q},\mathbf{u}) = \mathbf{B}(t,\mathbf{q})\mathbf{u} + \boldsymbol{\beta}(t,\mathbf{q}) \tag{121}$$

with $\mathbf{u}(t) \in \mathbb{R}^m$ and $\mathbf{B}(t,\mathbf{q}(t)) \in \mathbb{R}^{n\times m}$. Such a generalization is for example needed in rigid body dynamics, when the orientations of the bodies are described by unit quaternions and the components of the angular velocities with respect to a body fixed frame are chosen as velocity parameters of the system. Another prominent example is the use of minimal coordinates and minimal velocities for a nonholonomic system, where typically $m < n$.

It follows immediately from (121) that

$$\mathrm{d}\dot{\mathbf{q}} = \mathbf{B}(t,\mathbf{q})\mathrm{d}\mathbf{u} + \frac{\partial \dot{\mathbf{q}}(t,\mathbf{q},\mathbf{u})}{\partial \mathbf{q}}\mathrm{d}\mathbf{q} + \frac{\partial \dot{\mathbf{q}}(t,\mathbf{q},\mathbf{u})}{\partial t}\mathrm{d}t.$$

Gathering the densities with respect to $\mathrm{d}t$ after using (31) and (121) allows to rewrite the differential measure of $\dot{\mathbf{q}}$ as

$$\mathrm{d}\dot{\mathbf{q}} = \ddot{\mathbf{q}}(t,\mathbf{q},\mathbf{u},\mathbf{a})\mathrm{d}t + \mathbf{B}(t,\mathbf{q})(\mathbf{u}^+ - \mathbf{u}^-)\mathrm{d}\eta, \tag{122}$$

where we have introduced the function

$$\ddot{\mathbf{q}}(t,\mathbf{q},\mathbf{u},\mathbf{a}) = \mathbf{B}(t,\mathbf{q})\mathbf{a} + \frac{\partial \dot{\mathbf{q}}(t,\mathbf{q},\mathbf{u})}{\partial \mathbf{q}}\dot{\mathbf{q}}(t,\mathbf{q},\mathbf{u}) + \frac{\partial \dot{\mathbf{q}}(t,\mathbf{q},\mathbf{u})}{\partial t}. \tag{123}$$

It is straightforward to see, that after introducing the stabilization as in (62), we have

$$\begin{aligned} \mathrm{d}\mathbf{q} &= \dot{\mathbf{q}}(t,\mathbf{q},\mathbf{u}+\mathbf{u}_S)\mathrm{d}t, \\ \mathrm{d}\dot{\mathbf{q}} &= \ddot{\mathbf{q}}(t,\mathbf{q},\mathbf{u},\mathbf{a}+\mathbf{a}_S)\mathrm{d}t + \mathbf{B}(t,\mathbf{q})(\mathbf{u}^+ - \mathbf{u}^-)\mathrm{d}\eta. \end{aligned} \tag{124}$$

By a similar reasoning as in Section 5, we can arrive at the corresponding position update formula given as

$$\mathbf{q}_{i+1} = \mathbf{q}_i + \Delta t\, \dot{\mathbf{q}}(t_i,\mathbf{q}_i,\mathbf{u}_i) + \frac{\Delta t^2}{2}\ddot{\mathbf{q}}\left(t_i,\mathbf{q}_i,\mathbf{u}_i,(1-2\beta)\overline{\mathbf{a}}_i + 2\beta\overline{\mathbf{a}}_{i+1}\right) + \mathbf{B}(t_i,\mathbf{q}_i)\mathbf{Q}_{i+1}, \tag{125}$$

which generalizes the update formula (73).

9 | NUMERICAL IMPLEMENTATION

In this section we apply the ideas of Section 2.3 to the nonsmooth generalized-α method. As initial conditions of the stepping scheme, we assume that we know the values of the kinematic quantities $\mathbf{q}_0$, $\mathbf{u}_0$, $\mathbf{a}_0$, $\mathbf{U}_0$, and $\mathbf{Q}_0$ as well as all

discrete forces at the initial time t_0. The initial conditions must be compatible in the sense that they solve the discrete equations of motion as well as satisfy all constraints at the initial time t_0. As initial value for the auxiliary variables we choose the first order approximation [*] $\overline{\mathbf{a}}_0 = \mathbf{a}_0$ and $\overline{\lambda}_{\square,0} = \lambda_{\square,0}$.

We assume the quantities at the beginning of the time step to be known and formulate the presented scheme as a system of nonlinear equations $\mathbf{R}(\mathbf{x}) = 0$, where

$$\mathbf{x}^{\mathrm{T}} = \left(\mathbf{a}_{i+1}^{\mathrm{T}}\ \mathbf{U}_{i+1}^{\mathrm{T}}\ \mathbf{Q}_{i+1}^{\mathrm{T}}\ \boldsymbol{\kappa}_{g,i+1}^{\mathrm{T}}\ \boldsymbol{\Lambda}_{g,i+1}^{\mathrm{T}}\ \boldsymbol{\lambda}_{g,i+1}^{\mathrm{T}}\ \boldsymbol{\Lambda}_{\gamma,i+1}^{\mathrm{T}}\ \boldsymbol{\lambda}_{\gamma,i+1}^{\mathrm{T}}\ \boldsymbol{\kappa}_{N,i+1}^{\mathrm{T}}\ \boldsymbol{\Lambda}_{N,i+1}^{\mathrm{T}}\ \boldsymbol{\lambda}_{N,i+1}^{\mathrm{T}}\ \boldsymbol{\Lambda}_{F,i+1}^{\mathrm{T}}\ \boldsymbol{\lambda}_{F,i+1}^{\mathrm{T}}\right). \tag{126}$$

The nonlinear equations are then solved by a semismooth Newton method. The computed $\mathbf{x}$ can subsequently be used to find the remaining quantities at the end of the time step. Hence, the positions, velocities and percussions at t_{i+1} are regarded as dependent on $\mathbf{x}$. In fact, we can solve (71) for $\overline{\mathbf{a}}_{i+1}$ and use it to compute $\mathbf{q}_{i+1}$ and $\mathbf{u}_{i+1}$ from (73) or its generalized counterparts of Section 8. Similarly, the auxiliary contact forces can be computed from (96) and (114), respectively. In turn, these can be directly inserted into (102), (95), and (113) to retrieve the respective values of $\hat{\boldsymbol{\kappa}}_{N,i+1}$, $\mathbf{P}_{N,i+1}$ and $\mathbf{P}_{F,i+1}$.

Having in mind that the just mentioned quantities depend on $\mathbf{x}$, the first part of the residual $\mathbf{R}$ is stated as

$$\mathbf{R}_{\mathrm{s}} = \begin{pmatrix} \mathbf{M}_{i+1}\ \mathbf{a}_{i+1} - \mathbf{h}_{i+1} - \sum\limits_{\square\in\{g,\gamma,N,F\}} \mathbf{W}_{\square,i+1}\ \lambda_{\square,i+1} \\ \mathbf{M}_{i+1}\mathbf{U}_{i+1} - \sum\limits_{\square\in\{g,\gamma,N,F\}} \mathbf{W}_{\square,i+1}\ \boldsymbol{\Lambda}_{\square,i+1} \\ \mathbf{M}_{i+1}\mathbf{Q}_{i+1} - \sum\limits_{K\in\{g,N\}} \mathbf{W}_{K,i+1}\boldsymbol{\kappa}_{K,i+1} - \sum\limits_{R\in\{\gamma,F\}} \frac{\Delta t}{2}\mathbf{W}_{R,i+1}\boldsymbol{\Lambda}_{R,i+1} \\ \boldsymbol{g}(t_{i+1}, \mathbf{q}_{i+1}) \\ \dot{\boldsymbol{g}}(t_{i+1}, \mathbf{q}_{i+1}, \mathbf{u}_{i+1}) \\ \ddot{\boldsymbol{g}}(t_{i+1}, \mathbf{q}_{i+1}, \mathbf{u}_{i+1}, \mathbf{a}_{i+1}) \\ \boldsymbol{\gamma}(t_{i+1}, \mathbf{q}_{i+1}, \mathbf{u}_{i+1}) \\ \dot{\boldsymbol{\gamma}}(t_{i+1}, \mathbf{q}_{i+1}, \mathbf{u}_{i+1}, \mathbf{a}_{i+1}) \end{pmatrix}, \tag{127}$$

where we assumed a splitting of the residual $\mathbf{R} = (\mathbf{R}_{\mathrm{s}}^{\mathrm{T}}\ \mathbf{R}_{\mathrm{c}}^{\mathrm{T}})^{\mathrm{T}}$ into a part $\mathbf{R}_{\mathrm{s}}$ containing all equations except the discrete contact laws, which are contemplated in $\mathbf{R}_{\mathrm{c}}$. Hereby, we have chosen the subscript "s" for $\mathbf{R}_{\mathrm{s}}$ to indicate the smooth part of the residual. In order to state the remaining part of the residual, we have to formulate the normal cone inclusions arising in the discrete contact laws as equations. This is done using the results from Section 2.3 and gives a piecewise smooth residual $\mathbf{R}_{\mathrm{c}}^{\mathrm{T}} = (\mathbf{R}_{\kappa_N}^{\mathrm{T}}\ \mathbf{R}_{\Lambda_N}^{\mathrm{T}}\ \mathbf{R}_{\lambda_N}^{\mathrm{T}}\ \mathbf{R}_{\Lambda_F}^{\mathrm{T}}\ \mathbf{R}_{\lambda_F}^{\mathrm{T}})$, which we subsequently set up part by part.

We start with the normal contact law on position level (101) and use (22) to restate the law as

$$\hat{\kappa}_{N,i+1}^{k} = -\mathrm{prox}_{\mathbb{R}_0^-}\left(r g_{N,i+1}^{k} - \hat{\kappa}_{N,i+1}^{k}\right) \quad k = 1, \ldots, n_N. \tag{128}$$

Equivalently, we can by (26) restate (101) as the residual

$$\begin{aligned} k \in \mathcal{A}_{i+1}: &\quad R_{\kappa_N}^{k} := g_{N,i+1}^{k} = 0 \\ k \in \overline{\mathcal{A}}_{i+1}: &\quad R_{\kappa_N}^{k} := \hat{\kappa}_{N,i+1}^{k} = 0, \end{aligned}$$

where we have implicitly defined the kth component $R_{\kappa_N}^{k}$ of $\mathbf{R}_{\kappa_N}$ and where we have introduced the set

$$\mathcal{A}_{i+1} = \left\{ k = 1, \ldots, n_N \;\middle|\; r g_{N,i+1}^{k} - \hat{\kappa}_{N,i+1}^{k} \le 0 \right\} \tag{130}$$

together with its complement $\overline{\mathcal{A}}_{i+1} = \{1, \ldots, n_N\} \setminus \mathcal{A}_{i+1}$.

[*] A more accurate initialization can be found on page 351 in Reference 13.

Since for contacts in $\mathcal{A}_{i+1}$ we are demanding the gap to be closed at the end of the time step, see (129), we have that $\mathcal{A}_{i+1}$ contains the same contacts as A_{i+1} because due to the stabilization no contact is penetrated at the end of the time step. We can use this fact to state the residual for the contact law on velocity level.

We use again (26) to formulate the normal contact law (94) as

$$\begin{aligned} k \in \mathcal{A}_{i+1} : \quad & P^k_{N,i+1} = -\text{prox}_{\mathbb{R}^-_0}\left(r\xi^k_{N,i+1} - P^k_{N,i+1}\right) \\ k \in \overline{\mathcal{A}}_{i+1} : \quad & P^k_{N,i+1} = 0. \end{aligned} \tag{131}$$

Similar to before, the kth component $R^k_{\Lambda_N}$ of $\mathbf{R}_{\Lambda_N}$ follows from (26) as

$$\begin{aligned} k \in \mathcal{B}_{i+1} : \quad & R^k_{\Lambda_N} := \xi^k_{N,i+1} = 0 \\ k \in \overline{\mathcal{B}}_{i+1} : \quad & R^k_{\Lambda_N} := P^k_{N,i+1} = 0, \end{aligned} \tag{132}$$

where we have introduced the set

$$\mathcal{B}_{i+1} = \left\{ k \in \mathcal{A}_{i+1} \;\middle|\; r\xi^k_{N,i+1} - P^k_{N,i+1} \leq 0 \right\} \tag{133}$$

as well as its complement $\overline{\mathcal{B}}_{i+1} = \{1, \dots, n_N\} \setminus \mathcal{B}_{i+1}$. Since, $\mathcal{B}_{i+1}$ is the subset of closed contacts $\mathcal{A}_{i+1}$ for which by (132) $\xi^k_{N,i+1} = 0$, the set $\mathcal{B}_{i+1}$ and B_{i+1} contain the same contacts. The reasoning here is similar as on position level.

Finally, we can proceed in the same manner with the acceleration level constraint (87) and state it as

$$\begin{aligned} k \in \mathcal{B}_{i+1} : \quad & \lambda^k_{N,i+1} = -\text{prox}_{\mathbb{R}^-_0}\left(r\ddot{g}^k_{N,i+1} - \lambda^k_{N,i+1}\right) \\ k \in \overline{\mathcal{B}}_{i+1} : \quad & \lambda^k_{N,i+1} = 0. \end{aligned} \tag{134}$$

With this intermediate step, the k-th component $R^k_{\lambda_N}$ of $\mathbf{R}_{\lambda_N}$ is then implicitly defined by

$$\begin{aligned} k \in \mathcal{C}_{i+1} : \quad & R^k_{\lambda_N} := \ddot{g}^k_{N,i+1} = 0 \\ k \in \overline{\mathcal{C}}_{i+1} : \quad & R^k_{\lambda_N} := \lambda^k_{N,i+1} = 0, \end{aligned} \tag{135}$$

where we have introduced the set

$$\mathcal{C}_{i+1} = \left\{ k \in \mathcal{B}_{i+1} \;\middle|\; r\ddot{g}^k_{N,i+1} - \lambda^k_{N,i+1} \leq 0 \right\} \tag{136}$$

as well as its complement $\overline{\mathcal{C}}_{i+1} = \{1, \dots, n_N\} \setminus \mathcal{C}_{i+1}$. Again, due to the stabilization and (135), the sets $\mathcal{C}_{i+1}$ and C_{i+1} contain the same contacts along the discrete motion.

For the discrete friction laws the procedure is the same and we start with reformulating (112) as

$$\begin{aligned} k \in \mathcal{A}_{i+1} : \quad & \mathbf{P}^k_{F,i+1} = -\text{prox}_{C_F(P^k_{N,i+1})}\left(r\boldsymbol{\xi}^k_{F,i+1} - \mathbf{P}^k_{F,i+1}\right) \\ k \in \overline{\mathcal{A}}_{i+1} : \quad & \mathbf{P}^k_{F,i+1} = 0, \end{aligned} \tag{137}$$

where we used (22). We can now use (27) to implicitly define the k-th contribution of the residual $\mathbf{R}^{\mathrm{T}}_{\Lambda_F} = \left((\mathbf{R}^1_{\Lambda_F})^{\mathrm{T}} \dots (\mathbf{R}^{n_N}_{\Lambda_F})^{\mathrm{T}}\right)$ as

$$\begin{aligned} k \in \mathcal{D}^{\mathrm{st}}_{i+1} : \quad & \mathbf{R}^k_{\Lambda_F} := \boldsymbol{\xi}^k_{F,i+1} = 0, \\ k \in \mathcal{D}^{\mathrm{sl}}_{i+1} : \quad & \mathbf{R}^k_{\Lambda_F} := \mathbf{P}^k_{F,i+1} + \mu^k P^k_{N,i+1} \frac{\boldsymbol{\xi}^k_{F,i+1}}{\|\boldsymbol{\xi}^k_{F,i+1}\|} = 0, \\ k \in \overline{\mathcal{A}}_{i+1} : \quad & \mathbf{R}^k_{\Lambda_F} := \mathbf{P}^k_{F,i+1} = 0, \end{aligned} \tag{138}$$

where we have introduced the sets

$$\mathcal{D}_{i+1}^{\mathrm{st}} = \left\{ k \in \mathcal{A}_{i+1} \;\middle|\; r\boldsymbol{\xi}_{F,i+1}^{k} - \mathbf{P}_{F,i+1}^{k} \in C_F(P_{N,i+1}^{k}) \right\} \tag{139}$$

and $\mathcal{D}_{i+1}^{\mathrm{sl}} = \mathcal{A}_{i+1} \setminus \mathcal{D}_{i+1}^{\mathrm{st}}$. Again it is clear from (138) that the set $\mathcal{D}_{i+1}^{\mathrm{st}}$ corresponds the set of sticking contacts D_{i+1}^{st} and consequently $\mathcal{D}_{i+1}^{\mathrm{sl}}$ to the set of slipping contacts D_{i+1}^{sl}. This, together with (22), allows to rewrite (117) as

$$\begin{aligned} k \in \mathcal{D}_{i+1}^{\mathrm{st}} &: \quad \lambda_{F,i+1}^{k} = -\mathrm{prox}_{C_F(\lambda_{N,i+1}^{k})}\left(r\dot{\boldsymbol{\gamma}}_{F,i+1}^{k} - \lambda_{F,i+1}^{k} \right), \\ k \in \mathcal{D}_{i+1}^{\mathrm{sl}} &: \quad \lambda_{F,i+1}^{k} = -\mu^k \lambda_{N,i+1}^{k} \frac{\boldsymbol{\gamma}_{F,i+1}^{k}}{\|\boldsymbol{\gamma}_{F,i+1}^{k}\|}, \\ k \in \overline{\mathcal{A}}_{i+1} &: \quad \lambda_{F,i+1}^{k} = 0. \end{aligned} \tag{140}$$

We gather the sticking contacts which are also sticking on acceleration level by

$$\mathcal{E}_{i+1}^{\mathrm{st}} = \left\{ k \in \mathcal{D}_{i+1}^{\mathrm{st}} \;\middle|\; r\dot{\boldsymbol{\gamma}}_{F,i+1}^{k} - \lambda_{F,i+1}^{k} \in C_F(\lambda_{N,i+1}^{k}) \right\} \tag{141}$$

and define $\mathcal{E}_{i+1}^{\mathrm{sl}} = \mathcal{D}_{i+1}^{\mathrm{st}} \setminus \mathcal{E}_{i+1}^{\mathrm{st}}$. Consequently, (27) allows to reformulate (140) as

$$\begin{aligned} k \in \mathcal{E}_{i+1}^{\mathrm{st}} &: \quad \mathbf{R}_{\lambda_F}^{k} := \dot{\boldsymbol{\gamma}}_{F,i+1}^{k} = 0, \\ k \in \mathcal{E}_{i+1}^{\mathrm{sl}} &: \quad \mathbf{R}_{\lambda_F}^{k} := \lambda_{F,i+1}^{k} + \mu^k \lambda_{N,i+1}^{k} \frac{\dot{\boldsymbol{\gamma}}_{F,i+1}^{k}}{\|\dot{\boldsymbol{\gamma}}_{F,i+1}^{k}\|} = 0, \\ k \in \mathcal{D}_{i+1}^{\mathrm{sl}} &: \quad \mathbf{R}_{\lambda_F}^{k} := \lambda_{F,i+1}^{k} + \mu^k \lambda_{N,i+1}^{k} \frac{\boldsymbol{\gamma}_{F,i+1}^{k}}{\|\boldsymbol{\gamma}_{F,i+1}^{k}\|} = 0, \\ k \in \overline{\mathcal{A}}_{i+1} &: \quad \mathbf{R}_{\lambda_F}^{k} := \lambda_{F,i+1}^{k} = 0, \end{aligned} \tag{142}$$

where we implicitly defined the kth contribution of the residual $\mathbf{R}_{\lambda_F}^{\mathrm{T}} = \left((\mathbf{R}_{\lambda_F}^{1})^{\mathrm{T}} \; \dots \; (\mathbf{R}_{\lambda_F}^{n_N})^{\mathrm{T}} \right)$.

Now that we have defined the residual $\mathbf{R}$, we can see that it is piecewise smooth, that is, it is smooth (differentiable) in $\mathbf{x}$ if the index sets $\mathcal{A}_{i+1}, \mathcal{B}_{i+1}, \dots$ do not change in the vicinity of $\mathbf{x}$. This enables us to use a semismooth Newton method to solve $\mathbf{R}(\mathbf{x}) = 0$. Hence, a time step of the scheme can be summarized as follows:

Time step with semismooth Newton method:

1. As starting value ($\nu = 0$) we use the vector $\mathbf{x}^0$ constructed like (126) but by choosing the known values at the beginning of the time step.
2. While $\|\mathbf{R}(\mathbf{x}^\nu)\|_\infty \leq \mathrm{TOL_n}$ and $\nu \leq \mathrm{MAXITER_n}$ do the Newton update

$$\mathbf{x}^{\nu+1} = \mathbf{x}^{\nu} - \nabla\mathbf{R}(\mathbf{x}^{\nu})^{-1}\mathbf{R}(\mathbf{x}^{\nu}) \tag{143}$$

   and increase ν by one. Hereby, $\nabla\mathbf{R}(\mathbf{x}^\nu)$ denotes the Jacobian matrix of $\mathbf{R}$ evaluated at $\mathbf{x}^\nu$, where the index sets $\mathcal{A}_{i+1}, \mathcal{B}_{i+1}, \dots$ are held constant (equal to the sets arising in the computation of $\mathbf{R}(\mathbf{x}^\nu)$) while taking the partial derivatives.
3. Solve (71) for $\overline{\mathbf{a}}_{i+1}$ and use it to compute $\mathbf{q}_{i+1}$ and $\mathbf{u}_{i+1}$ from (73) or its generalized counterparts of Section 8. Similarly, compute the auxiliary contact forces from (96) and (114), respectively and insert these into (102), (95), and (113) leading to $\hat{\boldsymbol{\kappa}}_{N,i+1}$, $\mathbf{P}_{N,i+1}$, and $\mathbf{P}_{F,i+1}$.

For the sake of completeness, we remark that step 3) is only needed for output purposes and is basically the first part of the computation of $\mathbf{R}$ in the subsequent time step. Moreover, it is clear from (143) that the Jacobian matrix $\nabla\mathbf{R}$ must have full rank.

For mechanical systems without friction, the here presented scheme is very similar to the generalized-α method presented in Reference 13. The only difference lies in the residuals describing the normal contact law on position and velocity level. Specifically, in Reference 13 the authors use $\kappa_{N,i+1}^{k} = 0$ instead of $\hat{\kappa}_{N,i+1}^{k} = 0$ in (129) as well as $\Lambda_{N,i+1}^{k} = 0$ instead of $P_{N,i+1}^{k} = 0$ in (132). Even though by our experience, this small difference produces if at all minimal differences in the

motion and the forces of the simulated system, it is more than just a subtlety. In fact, replacing the contact force quantities in (129) and (132) destroys the equivalence of the contact law formulated using the sets $\mathcal{A}_{i+1}$ and $\mathcal{B}_{i+1}$ with the corresponding discrete contact laws formulated as normal cone inclusions.

In cases where multiple contacts with linearly dependent generalized force directions are present in the system, the Jacobian matrix $\nabla\mathbf{R}$ is singular. Hence, for this kind of system the equation $\mathbf{R}(\mathbf{x}) = 0$ must be solved by a method that does not invert this Jacobian matrix. A popular choice is to reformulate the system $\mathbf{R}(\mathbf{x}) = 0$ such that it can be solved by fixed point iterations, see Section 2.3 and References 6,23. For the aforementioned reformulation, we split the vector of unknowns as $\mathbf{x}^{\mathrm{T}} = (\mathbf{y}^{\mathrm{T}}\ \mathbf{z}^{\mathrm{T}})$, where

$$\begin{aligned}\mathbf{y}^{\mathrm{T}} &= (\mathbf{a}_{i+1}^{\mathrm{T}}\ \mathbf{U}_{i+1}^{\mathrm{T}}\ \mathbf{Q}_{i+1}^{\mathrm{T}}\ \boldsymbol{\kappa}_{g,i+1}^{\mathrm{T}}\ \boldsymbol{\Lambda}_{g,i+1}^{\mathrm{T}}\ \boldsymbol{\lambda}_{g,i+1}^{\mathrm{T}}\ \boldsymbol{\Lambda}_{\gamma,i+1}^{\mathrm{T}}\ \boldsymbol{\lambda}_{\gamma,i+1}^{\mathrm{T}}),\\ \mathbf{z}^{\mathrm{T}} &= (\boldsymbol{\kappa}_{N,i+1}^{\mathrm{T}}\ \boldsymbol{\Lambda}_{N,i+1}^{\mathrm{T}}\ \boldsymbol{\lambda}_{N,i+1}^{\mathrm{T}}\ \boldsymbol{\Lambda}_{F,i+1}^{\mathrm{T}}\ \boldsymbol{\lambda}_{F,i+1}^{\mathrm{T}}).\end{aligned} \tag{144}$$

Since $\mathbf{y}$ does not contain any contact forces, $\frac{\partial \mathbf{R}_{\mathrm{s}}}{\partial \mathbf{y}}$ can be regular despite the presence of linearly dependent contact force directions. Assuming that this is the case, the implicit function theorem applied to $\mathbf{R}_{\mathrm{s}}(\mathbf{y}, \mathbf{z}) = 0$ states the existence of a function $\mathbf{F}$ such that $\mathbf{y} = \mathbf{F}(\mathbf{z})$, that is, we can regard $\mathbf{y}$ as depending on the contact forces at the end of the time step. Moreover, it can be seen from the derivation of the residual $\mathbf{R}_{\mathrm{c}}$ above, that it can be equivalently formulated as $\mathbf{z} = \mathbf{p}(\mathbf{y}, \mathbf{z})$, where $\mathbf{p}$ makes use of the proximal point function. Indeed, see for example that (129) is equivalent to (128) or that (138) is equivalent to (137). This leaves us with an equation $\mathbf{z} = \mathbf{p}(\mathbf{F}(\mathbf{z}), \mathbf{z})$, which we can solve using fixed point iterations.

Numerically, we can find the value $\mathbf{y} = \mathbf{F}(\mathbf{z})$ by solving $\mathbf{R}_{\mathrm{s}}(\mathbf{y}, \mathbf{z}) = 0$ for a fixed value of $\mathbf{z}$ using Newton's method. The computed value $\mathbf{y}$ in turn is then used in the fixed point iteration. Therefore, a time step of the scheme can be implemented as follows:

Time step with fixed point iterations:

1. As starting value ($\nu = \mu = 0$) we use the vectors $\mathbf{y}^0$ and $\mathbf{z}^0$ constructed like (144) but by choosing the known values at the beginning of the time step.
2. While $||\mathbf{z}^{\mu} - \mathbf{p}(\mathbf{y}^0, \mathbf{z}^{\mu})||_{\infty} \leq \mathrm{TOL}_{\mathrm{fp}}$ and $\mu \leq \mathrm{MAXITER}_{\mathrm{fp}}$ do the fixed point update

   (i) While $||\mathbf{R}_{\mathrm{s}}(\mathbf{y}^{\nu}, \mathbf{z}^{\mu})||_{\infty} \leq \mathrm{TOL}_{\mathrm{n}}$ and $\nu \leq \mathrm{MAXITER}_{\mathrm{n}}$, perform a Newton step

   $$\mathbf{y}^{\nu+1} = \mathbf{y}^{\nu} - \nabla_{\mathbf{y}}\mathbf{R}_{\mathrm{s}}(\mathbf{y}^{\nu}, \mathbf{z}^{\mu})^{-1}\mathbf{R}_{\mathrm{s}}(\mathbf{y}^{\nu}, \mathbf{z}^{\mu}) \tag{145}$$

   and increase ν by one. Hereby, $\nabla_{\mathbf{y}}\mathbf{R}_{\mathrm{s}}(\mathbf{y}^{\nu}, \mathbf{z}^{\mu})$ denotes the Jacobian matrix of $\mathbf{R}_{\mathrm{s}}$ with respect to its $\mathbf{y}$ dependence.

   (ii) Use the converged solution $\mathbf{y}^{\nu}$ of step (i) to perform the fixed point update

   $$\mathbf{z}^{\mu+1} = \mathbf{p}(\mathbf{y}^{\nu}, \mathbf{z}^{\mu}). \tag{146}$$

   Subsequently increase μ by one and set $\nu = 0$ as well as $\mathbf{y}^0 = \mathbf{y}^{\nu}$.

3. Solve (71) for $\overline{\mathbf{a}}_{i+1}$ and use it to compute $\mathbf{q}_{i+1}$ and $\mathbf{u}_{i+1}$ from (73) or its generalized counterparts of Section 8. Similarly, compute the auxiliary contact forces from (96) and (114), respectively and insert these into (102), (95), and (113) leading to $\hat{\boldsymbol{\kappa}}_{N,i+1}$, $\mathbf{P}_{N,i+1}$, and $\mathbf{P}_{F,i+1}$.

Last but not least, it has to be mentioned that the parameter r used in the prox-equations as well as in the index sets $\mathcal{A}_{i+1}, \mathcal{B}_{i+1}, \ldots$ could be chosen differently for every contact and even differently for the normal contact law and the friction law of the same contact.

10 | EXAMPLES

In this section we use the presented nonsmooth generalized-α scheme to obtain the time evolution of some benchmark systems, which are all chosen such that particular features of the scheme can be validated separately.

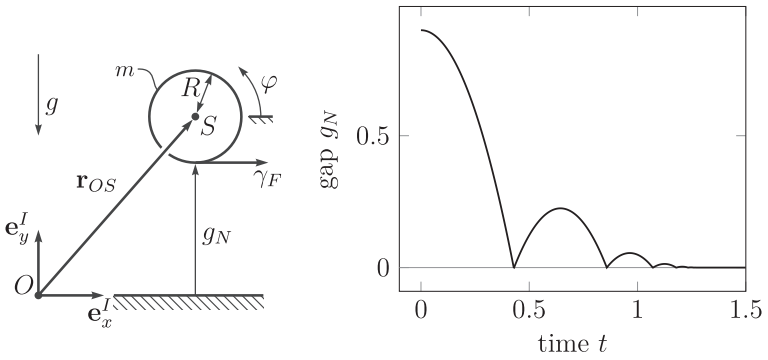

FIGURE 1 Sketch of the bouncing ball system (left) and simulated time evolution for the case where $\omega = 0$ and $e_N = 0.5$ (right)

10.1 | Rotating bouncing ball

Following References 33,34, we look at a homogeneous rigid sphere of radius $R = 0.1$ and mass $m = 1$ which is constrained to move in the $(\mathbf{e}_x^I$–$\mathbf{e}_y^I)$-plane and which under the influence of gravity with gravitational acceleration $g = 9.81$ falls on a horizontal plane, see Figure 1. To parametrize the motion of the ball, we choose the minimal coordinates $\mathbf{q} = (x\ y\ \varphi)^{\mathrm{T}}$, where the center of mass S of the sphere is addressed by the representation ${}_I\mathbf{r}_{OS} = (x\ y\ 0)^{\mathrm{T}}$ of the position vector $\mathbf{r}_{OS}$ with respect to the basis I. Moreover, the angle φ describes the orientation of the sphere. The velocity parameters $\mathbf{u} = (u_x\ u_y\ u_\varphi)^{\mathrm{T}}$ are chosen to correspond to $\dot{\mathbf{q}}$ whenever the time derivative of the coordinates exist. Consequently, we have

$$\mathbf{M} = \begin{pmatrix} m & 0 & 0 \\ 0 & m & 0 \\ 0 & 0 & \theta_S \end{pmatrix} \quad \text{and} \quad \mathbf{h} = \begin{pmatrix} 0 \\ -mg \\ 0 \end{pmatrix} \tag{147}$$

with the rotational inertia $\theta_S = \frac{2}{5}mR^2$ of the sphere. Finally, the contact with the plane is described by the gap function

$$g_N = y - R \quad \text{and} \quad \gamma_F = u_x + Ru_\varphi, \tag{148}$$

which is the relative horizontal velocity of the contact point with respect to the plane and with (49) describes planar Coulomb friction. We choose the friction coefficient $\mu = 0.2$ and the restitution coefficient $e_F = 0$.

To validate the presented scheme, three simulations are instructive. For all of them we choose $\mathbf{q}(0) = (0\ 1\ 0)^{\mathrm{T}}$ as initial configuration and use $\mathbf{u}(0) = (0\ 0\ \omega)^{\mathrm{T}}$, such that the ball has an initial rotational velocity ω.

The first case starts from rest, that is, $\omega = 0$, and we choose $e_N = 0.5$. This results in the typical bouncing motion, which exhibits the Zeno phenomenon. The simulation result† is shown in Figure 1 and asserts that the proposed scheme can overcome accumulation points.

The subsequent two cases are used to test the behavior of the scheme with respect to friction forces. For both cases, we set $e_N = 0$ implying that once the contact closes it remains closed, that is, the postimpact velocity is $u_y^+ = 0$, which allows us to validate friction. At the closing time instant a frictional impact occurs. Moreover, because the ball is constantly accelerated by gravitation, the preimpact velocity is $u_y^- = -\sqrt{2g(y(0) - R)}$. It then follows from the impact equations (53), that the impulsive normal contact force is $\Lambda_N = m\sqrt{2g(y(0) - R)} \approx 4.2$. Furthermore, after the impact the nonimpulsive normal contact force compensates the gravitational force and therefore takes the value $\lambda_N = mg = 9.81$. Depending on the value of ω, two cases arise.

In the first case, the rotational velocity is high, we choose $\omega = 50$, and the contact slides after the impact, implying that the friction forces attain the maximally allowed values $\Lambda_F = \mu\Lambda_N \approx 0.84$ and $\lambda_F = \mu\lambda_N \approx 1.96$. After a period of sliding contact, finally, the ball has slowed down enough such that a slip-stick transition takes place and the ball begins

†The generalized-α scheme with the following parameters was used: $r = 0.3$; $\Delta t = 2 \cdot 10^{-3}$; $\rho_\infty = 0.5$; $\mathrm{TOL}_{\mathrm{n}} = 10^{-6}$. The semismooth Newton method was used for all time steps and the Jacobian matrix $\nabla\mathbf{R}$ was computed by finite differences with a step size of $\varepsilon = 10^{-6}$. The maximal number of Newton steps (143) encountered in a time step was $\nu_{\max} = 1$ and the average was $\nu_{\mathrm{avg}} = 0.01$.

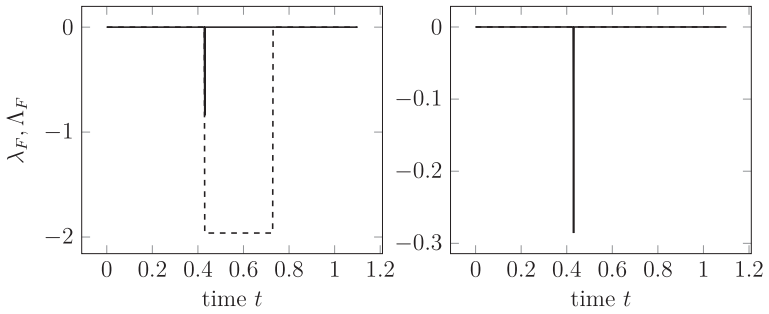

FIGURE 2 Simulated friction forces λ_F (dashed) and Λ_F (solid) for the cases $\omega = 50$ (left) and $\omega = 10$ (right)

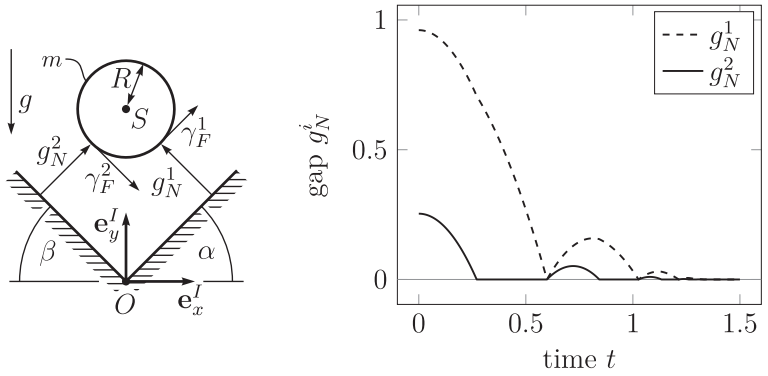

FIGURE 3 Sketch of the ball in corner system (left) and simulated time evolution of the gaps (right)

a pure rolling motion described by the kinematic condition $\gamma_F = 0$. Since the rolling motion is described by constant velocities, no net forces occur, implying $\lambda_F = 0$. Hence, at the slip-stick transition the nonimpulsive friction force instantly jumps to zero. Figure 2 shows that the described behavior of the friction forces is perfectly reproduced by the presented generalized-α scheme[2].

In the second case, when the rotational velocity is small enough, the contact sticks at impact and the ball exhibits a rolling motion directly after. As no friction force is needed for rolling, we have $\lambda_F = 0$ for all times. The preimpact velocities are $u_x^- = 0$ as well as $u_\varphi^- = \omega$. Since the contact sticks directly after the impact, that is, $\gamma_F^+ = 0$, from the impact equations (53) we can deduce that the impulsive friction force takes the value $\Lambda_F = -\frac{2}{7} mR\omega \approx -0.29$. Again this behavior is in perfect accordance with the simulation[†], see Figure 2.

10.2 | Ball in corner

A ball making frictional contact with a corner is a simple case where the Newton step (143) fails due to the singularity of the Jacobian matrix $\nabla \mathbf{R}$. Consider the ball described in Section 10.1 and assume it can get in contact with two inclined planes with inclination angles $\alpha = 45°$ and $\beta = 45°$, respectively, see Figure 3.

The gap functions and the friction velocities are

$$\boldsymbol{g}_N = \begin{pmatrix} -x\sin\alpha + y\cos\alpha - R \\ x\sin\beta + y\cos\beta - R \end{pmatrix} \quad \text{and} \quad \boldsymbol{\gamma}_F = \begin{pmatrix} u_x\cos\alpha + u_y\sin\alpha + ru_\varphi \\ u_x\cos\beta - u_y\sin\beta + ru_\varphi \end{pmatrix}. \tag{149}$$

For the simulation [‡]shown in Figure 3, we assumed the restitution coefficients to be $e_N^1 = 0.5$, $e_N^2 = 0$ and $e_F^1 = e_F^2 = 0$. For the friction coefficients we set $\mu^1 = \mu^2 = 0.3$. Starting at rest with $\mathbf{q}(0) = (-0.5\ 1\ 0)^{\mathrm{T}}$, the ball will eventually come

[‡]The generalized-α scheme with the following parameters was used: $r = 0.2$; $\Delta t = 10^{-4}$; $\rho_\infty = 0.5$; $\mathrm{TOL_n} = \mathrm{TOL_{fp}} = 10^{-6}$. The semismooth Newton method was used for all time steps, except for 13 time steps, where we had to switch to fixed-point iterations. The Jacobian matrix $\nabla \mathbf{R}$ was computed

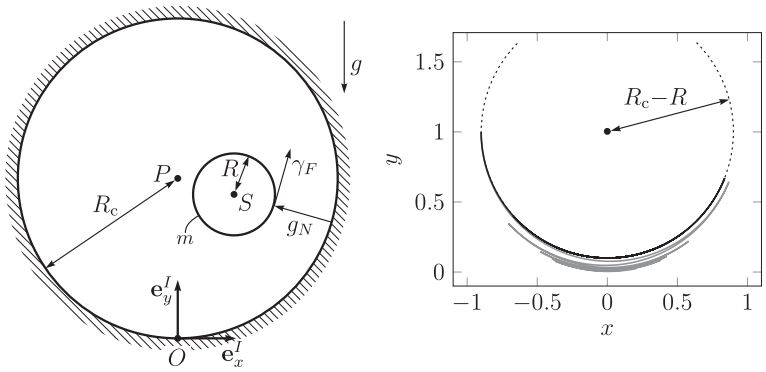

FIGURE 4 Sketch of the ball in cylinder system (left) and simulated time evolution of S (right). black: generalized-α scheme, gray: Moreau's time-stepping scheme

to rest with both contacts closed. It is exactly in that situation that the Jacobian matrix $\nabla\mathbf{R}$ becomes singular and the simulation can only be continued with fixed point iterations as solution strategy. In Figure 3, this is the case for $t \approx 1.36$.

10.3 | Ball in cylinder

The importance of the stabilization of the unilateral constraint at position level can impressively be shown by simulating the ball of Section 10.1 rolling inside a cylinder of radius $R_c = 1$. We assume that the centerline of the cylinder is orthogonal to the $\mathbf{e}_x^I$–$\mathbf{e}_y^I$-plane, such that it can be identified with the point P, see Figure 4.

The normal contact with the cylinder is described by the gap function

$$g_N = R_c - R - \|\mathbf{r}_{SP}\| \tag{150}$$

with $e_N = 0$. Using ${}_I\mathbf{n} = (n_x\ n_y\ 0)^T$ to denote the components of the inward normal $\mathbf{n} = \mathbf{r}_{SP}/\|\mathbf{r}_{SP}\|$ of the cylinder, we define the tangent unit vector ${}_I\mathbf{t} = (n_y\ -n_x\ 0)^T$. With that, we can define the tangent velocity

$$\gamma_F = {}_I\mathbf{v}_{SI}^T\mathbf{t} + Ru_\varphi, \tag{151}$$

where the velocity of S is ${}_I\mathbf{v}_S = (u_x\ u_y\ 0)^T$. We choose the friction coefficient $\mu = 0.1$ and the restitution coefficient $e_F = 0$. Looking at the trajectory of S simulated[§] with the generalized-α scheme shows that the contact does not penetrate. To show that contact penetration is a big issue for this system, we compared the trajectory of S resulting from the generalized-α scheme to the one gotten from a simulation[¶] with the widely used time-stepping scheme of Moreau,[1,6,35] which does not stabilize the unilateral constraint on position level. The comparison is shown in Figure 4. For the simulation we assume that the ball is initially at rest with $\mathbf{q}(0) = (-0.9\ 1\ 0)^T$.

10.4 | Painlevé rod

It is well known that during the sliding motion of rigid bodies over a rough surface, a "frictional dynamic catastrophe" can occur, that is, impulsive motion which is not the result of a collision. This phenomenon, called Painlevé paradox, is for example studied in References 33,36,37, where the following benchmark system is used.

by finite differences with a step size of $\varepsilon = 10^{-6}$. The maximal number of Newton steps (143) encountered in a time step was $\nu_{max} = 7$ and the average was $\nu_{avg} = 0.36$. The maximal number of fixed-point iterations (146) encountered in a time step was $\mu_{max} = 281$ and the average was $\mu_{avg} = 44.3$.

[§]The generalized-α scheme with the following parameters was used: $r = 0.3$; $\Delta t = 10^{-2}$; $\rho_\infty = 0.5$; $\mathrm{TOL_n} = 10^{-6}$. The semismooth Newton method was used for all time steps and the Jacobian matrix $\nabla\mathbf{R}$ was computed by finite differences with a step size of $\varepsilon = 10^{-6}$. The maximal number of Newton steps (143) encountered in a time step was $\nu_{max} = 74$ and the average was $\nu_{avg} = 0.37$.

[¶]Parameters for Moreau's time-stepping scheme: $r = 0.3$; $\Delta t = 10^{-2}$; $\mathrm{TOL_{fp}} = 10^{-6}$.

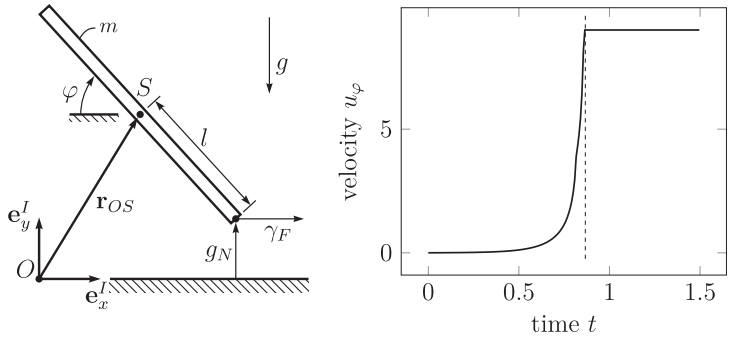

FIGURE 5 Sketch of the Painlevé rod (left) and simulated time evolution of the angular velocity of the rod (right)

Consider a rigid homogeneous slender rod of mass $m = 1$, length $2l$ and rotational inertia $\theta_S = \frac{1}{3}ml^2$, where $l = 1$. As shown in Figure 5, the rod moves in the $\mathbf{e}_x^I$–$\mathbf{e}_y^I$-plane and is under the influence of gravity with gravitational acceleration $g = 10$. Describing the orientation of the rod by the angle φ, we choose the minimal coordinates $\mathbf{q} = (x\ y\ \varphi)^{\mathrm{T}}$, where the center of mass S of the rod is addressed by ${}_I\mathbf{r}_{OS} = (x\ y\ 0)^{\mathrm{T}}$. Using the natural velocity coordinates $\mathbf{u}$ corresponding to $\dot{\mathbf{q}}$ almost everywhere, the mass matrix and the force vector of the system have the form (147). The contact of the rod's tip with the ground is described by

$$g_N = y - l\sin\varphi \quad \text{and} \quad \gamma_F = u_x - lu_\varphi \sin\varphi. \tag{152}$$

The friction coefficient is set to $\mu = 5/3$ and $e_N = e_F = 0$ is used to model inelastic impact behavior. With the initial conditions $\mathbf{q}(0) = (0\ l\sin(\varphi_0)\ \varphi_0)^{\mathrm{T}}$ and $\mathbf{u}(0) = (v\ 0\ 0)^{\mathrm{T}}$, the rod's tip is initially in contact and the rod slides with an initial inclination of $\varphi_0 = 31°$ and an initial horizontal velocity $v = 30$. As analyzed in Reference 33, this sliding motion eventually results in detaching of the contact. This detaching comes with a blowup of the accelerations and nonimpulsive contact forces, which is seen as an impact. The blowup of the accelerations leads to vertical asymptotes in the velocities, which constitute problems for integration schemes. However, since the asymptote is just an isolated singularity, event-capturing schemes with constant time step might overcome these blowups, as they do not try to fully resolve it. The simulation [#] result in Figure 5 shows that the presented generalize-α scheme can indeed deal with the Painlevé paradox.

10.5 | Guided hopper

The suitability of the presented nonsmooth generalized-α scheme for the simulation of flexible multibody systems is demonstrated by simulating a guided hopper. It consists of a vertically guided main body of mass $M = 3$, which is addressed by the coordinate y. At the hip H with ${}_I\mathbf{r}_{OH} = (x_0\ y\ 0)^{\mathrm{T}}$ a rigid homogeneous rod of mass $m = 1.56$, length $L = 0.2$, and rotational inertia $\theta_S = 8.5 \cdot 10^{-3}$ around the rod's center of mass is attached to the main body. x_0 is the arbitrary horizontal position of the guidance. The orientation of the rod is prescribed by the angle $\alpha(t)$ which is a given function of time. A straight planar Euler–Bernoulli beam[38] with undeformed length L is connected to the knee K of the rod by an actuated rotational joint with prescribed actuation angle $\beta(t)$ as a given function of time. For the linear elastic beam we choose the axial stiffness $EA = 1.89 \cdot 10^7$, the bending stiffness $EI = 14.2$ and the mass line density $\varrho = 0.71$. Moreover, we follow Reference 39 and discretize the centerline of the beam with B-Spline shape functions. Using the parameter $\xi \in [0, 1]$ to parametrize the beam and denoting the generalized coordinates of the beam by $\mathbf{q}_\mathrm{b}$, a point C on the centerline of the beam is addressed by $\mathbf{r}_{OC}(\xi, \mathbf{q}_\mathrm{b})$. We introduce the generalized coordinates $\mathbf{q} = (y\ \mathbf{q}_\mathrm{b}^{\mathrm{T}})^{\mathrm{T}}$ of the hopper as well as the auxiliary quantities $\mathbf{d} = \mathbf{r}_{OK} - \mathbf{r}_{OC}(0, \mathbf{q}_\mathrm{b})$ and $\varphi = \measuredangle(\mathbf{r}_{KH}, \mathbf{r}'_{OC}(0, \mathbf{q}_\mathrm{b}))$, where $(\cdot)'$ denotes the derivative with respect to ξ. With these quantities, the bilateral constraints composing the knee joint are

$$\boldsymbol{g} = \begin{pmatrix} \mathbf{e}_x^I \cdot \mathbf{d} \\ \mathbf{e}_y^I \cdot \mathbf{d} \\ \varphi - \beta \end{pmatrix}. \tag{153}$$

[#]The generalized-α scheme with the following parameters was used: $r = 0.1$; $\Delta t = 8 \cdot 10^{-4}$; $\rho_\infty = 0.9$; $\mathrm{TOL}_\mathrm{n} = 10^{-8}$. The semismooth Newton method was used for all time steps and the Jacobian matrix $\nabla\mathbf{R}$ was computed by finite differences with a step size of $\varepsilon = 10^{-6}$. The maximal number of Newton steps (143) encountered in a time step was $\nu_\mathrm{max} = 2$ and the average was $\nu_\mathrm{avg} = 0.07$.

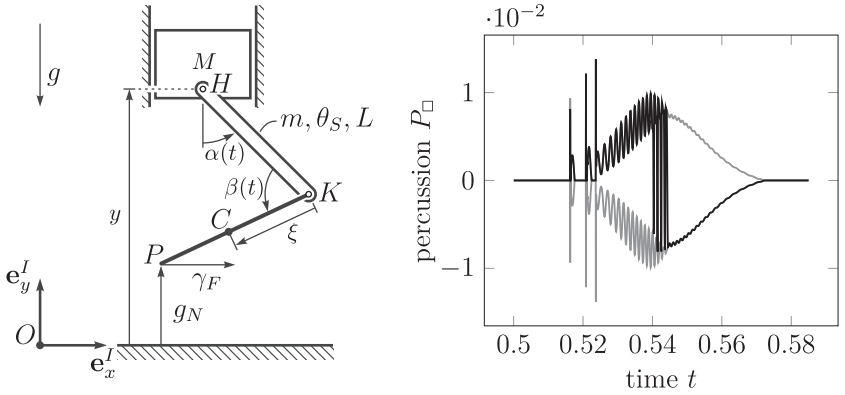

FIGURE 6 Sketch of the guided hopper (left) and simulated time evolution of the percussions (right). black: P_F, gray: $\pm\mu P_N$

Finally, the contact of the endpoint P of the beam with the horizontal plane is described by

$$g_N = \mathbf{e}_y^I \cdot \mathbf{r}_{OC}(1, \mathbf{q}_\mathrm{b}) \quad \text{and} \quad \gamma_F = \mathbf{e}_x^I \cdot \mathbf{v}_C(1, \mathbf{q}_\mathrm{b}, \dot{\mathbf{q}}_\mathrm{b}), \tag{154}$$

where $\mathbf{v}_C$ is the velocity of the centerline and corresponds to the time derivative of $\mathbf{r}_{OC}$ almost everywhere. The contact parameters are set to $e_N = e_F = 0$ and $\mu = 0.2$.

For the simulation,[‖] the system is initially assumed to be at rest with $y(0) = 0.31$. Moreover, the beam is undeformed initially. For the actuation angles

$$\alpha(t) = \frac{\pi}{3} - \frac{\pi}{30}\left(1 - \cos(4\pi\, t)\right) \quad \text{and} \quad \beta(t) = \pi - 2\alpha(t) \tag{155}$$

have been chosen and gravity is contemplated by the gravitational acceleration $g = 9.81$. The percussions, plotted in Figure 6, show that the generalized-α scheme can cope with the complex contact dynamics arising in multibody systems containing flexible parts and time dependent bilateral constraints. This makes the presented scheme well suited for engineering applications.

10.6 | Tippe top

The tippe top consists of a spherical main body at which a stick is attached. Starting from the standing position with stick pointing up and with high spinning velocity around its symmetry axis, the top inverts and spins on the stick. Since the spinning velocity decreases due to dissipation, the top tumbles back to the standing position after a while.

Let $R_1 = 1.5 \cdot 10^{-2}$ be the radius of the sphere with center C_1 characterizing the main body of the top. The rounded end of the stick is described by a sphere of radius $R_2 = 5 \cdot 10^{-3}$ and midpoint C_2. The two midpoints as well as the top's center of mass S lie on the axis of symmetry of the top and the distances between S and the points C_1 and C_2 are $a_1 = 3 \cdot 10^{-3}$ and $a_2 = 1.6 \cdot 10^{-2}$, respectively, see Figure 7. We describe the position of the top by the components ${}_I\mathbf{r}_{OS}$ of the position vector of S with respect to the resting basis I. To characterize the orientation of the top, we introduce the body fixed K-frame such that $\mathbf{e}_z^K$ lies on the symmetry axis of the top and points toward the stick. The transformation matrix $\mathbf{A}_{IK} = ({}_I\mathbf{e}_x^K\, {}_I\mathbf{e}_y^K\, \mathbf{e}_z^K)$ is then parametrized using a unit quaternion $\mathbf{p}$. Hence, the configuration of the top is described by $\mathbf{q} = ({}_I\mathbf{r}_{OS}^\mathrm{T}\ \mathbf{p}^\mathrm{T})^\mathrm{T}$. As generalized velocities we choose $\mathbf{u} = ({}_I\mathbf{v}_{SK}^\mathrm{T}\boldsymbol{\Omega}^\mathrm{T})^\mathrm{T}$ composed by the representations of the velocity $\mathbf{v}_S$ of S and the angular velocity of the top $\boldsymbol{\Omega}$ with respect to the bases I and K, respectively. As mentioned in Section 8, this choice leads to a model with the generalized kinematic equation (121). For the relevant quantities $\mathbf{B}$, $\boldsymbol{\beta}$, $\mathbf{M}$, and $\mathbf{h}$ describing a so parameterized rigid body under the influence of gravity, we refer to Reference 40.

[‖]The generalized-α scheme with the following parameters was used: $r = 0.15$; $\Delta t = 5 \cdot 10^{-5}$; $\rho_\infty = 0$; $\mathrm{TOL}_\mathrm{n} = 10^{-6}$. The beam was discretized by two elements of polynomial degree 2 and 5 Gauss quadrature points were used. The semismooth Newton method was used for all time steps and the Jacobian matrix $\nabla\mathbf{R}$ was computed analytically. The maximal number of Newton steps (143) encountered in a time step was $\nu_\mathrm{max} = 5$ and the average was $\nu_\mathrm{avg} = 1.23$.

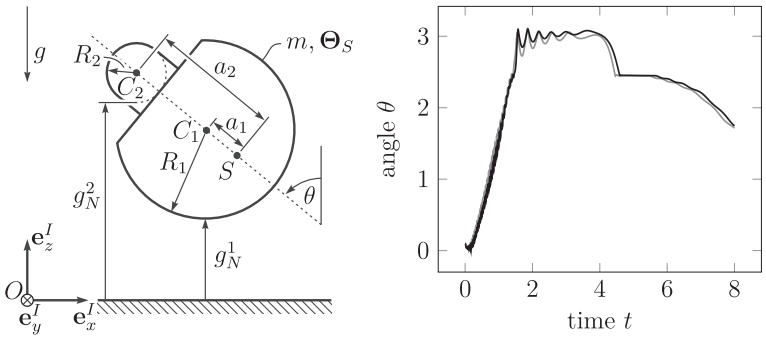

FIGURE 7 Sketch of the tippe top (left) and simulated time evolution of the angle θ (right). Black: presented model, gray: Reference 41

The mass of the top is $m = 6 \cdot 10^{-3}$ and the representation of the inertia tensor is the diagonal matrix ${}_K\boldsymbol{\Theta}_S = \operatorname{diag}(I_1, I_1, I_3)$ with $I_1 = 8 \cdot 10^{-7}$ and $I_3 = 7 \cdot 10^{-7}$.

To describe the contact between the ground and either the main body ($k = 1$) or the stick ($k = 2$), we use the gap

$$g_N^k = \mathbf{e}_z^I \cdot \mathbf{r}_{OC_k} - R_k. \tag{156}$$

The friction between the top and the ground is modeled as Coulomb–Contensou friction,[30] which uses the $n_F^k = 3$ velocity parameters

$$\boldsymbol{\gamma}_F^k = \begin{pmatrix} \mathbf{e}_x^I \cdot \mathbf{v}_{P_k} \\ \mathbf{e}_y^I \cdot \mathbf{v}_{P_k} \\ \frac{3\pi R}{16} \mathbf{e}_z^I \cdot \boldsymbol{\Omega} \end{pmatrix}, \tag{157}$$

where $\mathbf{v}_{P_k} = \mathbf{v}_{C_k} - R_k \boldsymbol{\Omega} \times \mathbf{e}_z^I$ denotes the velocity of the respective contact point and $R = 5 \cdot 10^{-4}$ denotes the assumed contact radius. This friction model assumes that the normal contact force λ_N^k stems from a parabolic force distribution over a circular contact area of radius R. A closer look at the velocity parameters (157) reveals that the first two velocities correspond to tangential contact velocities and capture translational Coulomb friction. Moreover, the third component is a representative radial contact velocity, which accounts for drilling friction. It is shown in Reference 41 that using the friction velocity (157) together with the set of admissible friction forces (49) results in a good approximation for the Coulomb–Contensou friction law used for the tippe top simulation in Reference 30.

For the simulation, [**] the top is initially at the position ${}_I\mathbf{r}_{OS}(0) = (0\ 0\ z_0)^{\mathrm{T}}$ with $z_0 = 1.2015 \cdot 10^{-2}$ and is inclined by the angle $\theta(0) = 0.1$, where θ denotes the angle between $\mathbf{e}_z^I$ and $\mathbf{e}_z^K$, that is, $\mathbf{e}_z^I \cdot \mathbf{e}_z^K = \cos\theta$. The center of mass S is assumed at rest and the top spins with initial angular velocity ${}_K\boldsymbol{\Omega} = (0\ 0\ 180)^{\mathrm{T}}$. To assure that the quaternion $\mathbf{p}$ remains a unit-quaternion, $\mathbf{p}$ is normalized after every step.

It is apparent from Figure 7 that the simulation results using the presented scheme are in line with the results of Reference 41 [††]. This shows that the presented scheme is well suited for mechanical systems with spatial friction as well as models with a general kinematic equation (121).

11 | CONCLUSION

We presented a nonsmooth generalized-α method for the simulation of mechanical systems with frictional contact. The dynamics of such systems, which additionally to the contacts can be subjected to ideal bilateral constraints, is described within the theory of nonsmooth mechanics. We have modeled the frictional contact as unilateral constraints

[**]The generalized-α scheme with the following parameters was used: $r = 0.001$; $\Delta t = 1 \cdot 10^{-3}$; $\rho_\infty = 0.5$; $\mathrm{TOL}_{\mathrm{n}} = 10^{-6}$. The semismooth Newton method was used for all time steps and the Jacobian matrix $\nabla\mathbf{R}$ was computed by finite differences with a step size of $\varepsilon = 10^{-6}$. The maximal number of Newton steps (143) encountered in a time step was $\nu_{\max} = 3$ and the average was $\nu_{\mathrm{avg}} = 0.36$.

[††]To reproduce the result of Reference 41 with Moreau's time-stepping scheme, we used: $r = 0.001$; $\Delta t = 1 \cdot 10^{-4}$; $\mathrm{TOL}_{\mathrm{fp}} = 10^{-6}$.

described by Signorini's law, the generalized Newton's impact law and a Coulomb-type friction law. All these laws are formulated as normal cone inclusions, allowing for a coherent discretization of the contact laws. All constraints are formulated on acceleration level and a numerical constraint drift, and hence contact penetration, is avoided by stabilizing the constraints on velocity and position level using the Gear–Gupta–Leimkuhler approach. The stabilized dynamics is discretized using generalized-α quadratures, which leads to a second-order accurate scheme during impact-free time intervals. Exploiting particular properties of the normal cone enabled to directly discretize the contact laws leading to their discrete counterparts, which depend on the discrete kinematic and kinetic quantities arising from the generalized-α discretization of the dynamics. The resulting time-stepping scheme still contains normal cone inclusions, which we have proposed to numerically treat by either a semismooth Newton method or by fixed point iterations. Finally, the derived nonsmooth generalized-α method has been validated using a set of mechanical benchmark systems.

The main contribution of this article is the extension of the nonsmooth generalized-α schemes[11-14] to systems with frictional contact and general kinematic equations. This has been achieved by formulating the set-valued Coulomb-type friction on velocity and acceleration level. Moreover, we have introduced the discrete contact laws as normal cone inclusions, which are shown to be a convenient interface to the numerical implementation of the scheme. Last but not least, we have devised a collection of benchmark systems suitable for validating the performance of any numerical scheme for mechanical systems with frictional contact, where every benchmark lies the focus on a different characteristics of such systems or of the numerical scheme. These characteristics are accumulation points, slip-stick transitions, the presence of linearly dependent force directions, contact penetration, the Painlevé paradox, the suitability of the scheme for the simulation of flexible multibody systems, combined spatial friction laws and general kinematic equations. We showed that the presented nonsmooth generalized-α scheme performs very well for all benchmark systems and hence qualifies for a broad range of engineering applications.

In fact, the presented scheme can reproduce the dynamics of a frictional contact adequately. Moreover, it performs well for multibody systems containing flexible parts and allows general parametrizations such as the use of unit quaternions for the rotation of rigid bodies.

DATA AVAILABILITY STATEMENT

Data are available upon request from the authors.

ORCID

Giuseppe Capobianco https://orcid.org/0000-0002-2384-2441
Simon R. Eugster https://orcid.org/0000-0002-4562-1287

REFERENCES

1. Moreau JJ. Unilateral contact and dry friction in finite freedom dynamics. In: Moreau JJ, Panagiotopoulos PD, eds. *Non-Smooth Mechanics and Applications. CISM Courses and Lectures*. Springer; 1988:1-82.
2. Glocker Ch. *Set-Valued Force Laws: Dynamics of Non-Smooth Systems. Lecture Notes in Applied Mechanics*. Vol 1. Springer; 2001.
3. Möller M. *Consistent Integrators for Non-Smooth Dynamical Systems*. PhD thesis. ETH Zurich; 2011.
4. Capobianco G., Eugster S. R. Time finite element based Moreau-type integrators. *International Journal for Numerical Methods in Engineering*. 2018;114(3):215–231.
5. Acary V. Higher order event capturing time-stepping schemes for nonsmooth multibody systems with unilateral constraints and impacts. *Appl Numer Math*. 2012;62:1259-1275.
6. Studer C. *Numerics of Unilateral Contacts and Friction: Modeling and Numerical Time Integration in Non-smooth Dynamics. Lecture Notes in Applied and Computational Mechanics*. Vol 47. Springer; 2009.
7. Schindler T, Acary V. Timestepping schemes for nonsmooth dynamics based on discontinuous Galerkin methods: definition and outlook. *Math Comput Simul*. 2014;95:180-199.
8. Gear CW, Leimkuhler B, Gupta GK. Automatic integration of Euler-Lagrange equations with constraints. *J Comput Appl Math*. 1985;12:77-90.
9. Acary V. Projected event-capturing time-stepping schemes for nonsmooth mechanical systems with unilateral contact and Coulomb's friction. *Comput Methods Appl Mech Eng*. 2013;256:224-250.
10. Schoeder S, Ulbrich H, Schindler T. Discussion of the gear–Gupta–Leimkuhler method for impacting mechanical systems. *Multibody Syst Dyn*. 2014;31(4):477-495.
11. Chen Q-Z, Acary V, Virlez G, Brüls O. A nonsmooth generalized-α scheme for flexible multibody systems with unilateral constraints. *Int J Numer Methods Eng*. 2013;96(8):487-511.
12. Brüls O, Acary V, Cardona A. Simultaneous enforcement of constraints at position and velocity levels in the nonsmooth generalized-α scheme. *Comput Methods Appl Mech Eng*. 2014;281:131-161.

13. Brüls O, Acary V, Cardona A. On the constraints formulation in the nonsmooth generalized-α method. *Advanced Topics in Nonsmooth Dynamics*. Springer; 2018:335-374.
14. Cosimo A, Galvez J, Cavalieri FJ, Cardona A, Brüls O. A robust nonsmooth generalized-α scheme for flexible systems with impacts. *Multibody Syst Dyn*. 2020;48(2):127-149.
15. Hilber HM, Hughes TJR, Taylor RL. Improved numerical dissipation for time integration algorithms in structural dynamics. *Earthq Eng Struct Dyn*. 1977;5(3):283-292.
16. Chung J, Hulbert G. A time integration algorithm for structural dynamics with improved numerical dissipation: the generalized-α method. *J Appl Mech*. 1993;60(2):371-375.
17. Arnold M, Brüls O. Convergence of the generalized-α scheme for constrained mechanical systems. *Multibody Syst Dyn*. 2007;18(2):185-202.
18. Galvez J, Cavalieri FJ, Cosimo A, Brüls O, Cardona A. A nonsmooth frictional contact formulation for multibody system dynamics. *Int J Numer Methods Eng*. 2020;121(16):3584-3609.
19. Cosimo A, Cavalieri FJ, Galvez J, Cardona A, Brüls O. A general purpose formulation for nonsmooth dynamics with finite rotations: application to the woodpecker toy. *J Comput Nonlinear Dyn*. 2021;16(3):031001.
20. Acary V, Brémond M, Huber O. On solving contact problems with Coulomb friction: formulations and numerical comparisons. *Advanced Topics in Nonsmooth Dynamics*. Springer; 2018:375-457.
21. Rockafellar RT, Wets R-B. *Variational Analysis*. Springer; 2009.
22. Leine RI, Nijmeijer H. *Dynamics and Bifurcations of Non-Smooth Mechanical Systems. Lecture Notes in Applied and Computational Mechanics*. Vol 18. Springer; 2004.
23. Alart P, Curnier A. A mixed formulation for frictional contact problems prone to Newton like solution methods. *Comput Methods Appl Mech Eng*. 1991;92:353-375.
24. De Giorgi E, Ambrosio L. Un nuovo tipo di funzionale del calcolo delle variazioni. *Atti della Accademia Nazionale dei Lincei. Classe di Scienze Fisiche, Matematiche e Naturali. Rendiconti Lincei. Matematica e Applicazioni*. 1988;82(2):199-210.
25. Ambrosio L, Fusco N, Pallara D. *Functions of Bounded Variation and Free Discontinuity Problems. Oxford Mathematical Monographs*. Clarendon Press; 2000.
26. Alberti G, Mantegazza C. A note on the theory of SBV functions. *Bollettino Unione Matematica Italiana*. 1997;11:375-382.
27. Leine RI, van de Wouw N. *Stability and Convergence of Mechanical Systems with Unilateral Constraints. Lecture Notes in Applied and Computational Mechanics*. Vol 36. Springer-Verlag; 2008.
28. Winandy T, Baumann M, Leine RI. Variational analysis of inequality impact laws for perfect unilateral constraints. *Advanced Topics in Nonsmooth Dynamics*. Springer; 2018:47-92.
29. Glocker Ch. Energetic consistency conditions for standard impacts. Part I: Newton-type inequality impact laws and Kane's example. *Multibody Syst Dyn*. 2013;29(1):77-117.
30. Leine RI, Glocker Ch. A set-valued force law for spatial Coulomb–Contensou friction. *Eur J Mech A/Solids*. 2003;22:193-216.
31. Newmark NM. A method of computation for structural dynamics. *J Eng Mech Div*. 1959;85(3):67-94.
32. Hairer E, Wanner G. *Solving Ordinary Differential Equations II*. 2nd ed. Springer; 2002.
33. Glocker Ch. Dynamik von Starrkörpersystemen mit Reibung und Stößen. PhD thesis. TU München; 1995.
34. Pfeiffer F, Glocker Ch. Contacts in multibody systems. *J Appl Math Mech*. 2000;64(5):773-782.
35. Glocker Ch. Simulation of hard contacts with friction: an iterative projection method. *Proceedings of a Conference in Honor of Jurgen Scheurle*. Springer; 2013.
36. Leine RI, Brogliato B, Nijmeijer H. Periodic motion and bifurcations induced by the Painlevé paradox. *Eur J Mech A/Solids*. 2002;21(5):869-896.
37. Génot F, Brogliato B. New results on Painlevé paradoxes. *Eur J Mech A/Solids*. 1999;18(4):653-677.
38. Eugster SR, Harsch J. *A Variational Formulation of Classical Nonlinear Beam Theories*. Springer International Publishing; 2020:95-121.
39. Harsch J, Eugster SR. *Finite Element Analysis of Planar Nonlinear Classical Beam Theories*. Springer International Publishing; 2020:123-157.
40. Sailer S, Eugster SR, Leine RI. The tippedisk: a tippetop without rotational symmetry. *Regul Chaotic Dyn*. 2020;25(6):553-580.
41. Möller M, Leine RI & Glocker Ch. An efficient approximation of orthotropic set-valued force laws of normal cone type. Proceedings of the 7th Euromech Solid Mechanics Conference, Lisbon; 2009:7-11.

How to cite this article: Capobianco G, Harsch J, Eugster SR, Leine RI. A nonsmooth generalized-alpha method for mechanical systems with frictional contact. *Int J Numer Methods Eng*. 2021;122:6497-6526. https://doi.org/10.1002/nme.6801